

1 **Phytohormonal cross-talk modulate *Bipolaris sorokiniana* (Sec.)interaction with Zea**  
2 **mays**

3 Muhammad Junaid Yousaf<sup>1</sup>, Anwar Hussain<sup>1\*</sup>, Muhammad Hamayun<sup>1</sup>, Amjad Iqbal<sup>2</sup>,  
4 Muhammad Irshad<sup>1</sup>, Ayaz Ahmad<sup>3</sup> and In-Jung Lee<sup>4\*</sup>

5 <sup>1</sup>Department of Botany, Garden Campus, Abdul Wali Khan University Mardan, Khyber  
6 Pakhtunkhwa Pakistan

7 <sup>2</sup>Department of Agriculture, Garden Campus, Abdul Wali Khan University Mardan, Khyber  
8 Pakhtunkhwa Pakistan

9 <sup>3</sup>Department of Biotechnology, Garden Campus, Abdul Wali Khan University Mardan,  
10 Khyber Pakhtunkhwa Pakistan

11 <sup>4</sup>School of Applied Biosciences, College of Agriculture and Life Sciences, Kyungpook  
12 National University, Daegu, South Korea

13 \* **Correspondence:** Anwar Hussain ([drhussain@awkum.edu.pk](mailto:drhussain@awkum.edu.pk)): In-Jung Lee  
14 ([ijlee@knu.edu.kr](mailto:ijlee@knu.edu.kr))

15

16 **Abstract**

17 Besides acting as growth inducing molecule, Gibberellin (GA<sub>3</sub>) also confers the compatibility  
18 of microbial interactions with host. We inoculated 11 days old *Z. mays* seedlings grown under  
19 hydroponic conditions and high GA<sub>3</sub> levels with *Bipolaris sorokiniana* (BIPOL) at the spore  
20 density (SD) of OD<sub>0.6</sub>. The high level of GA<sub>3</sub> negatively affected the growth of the seedlings,  
21 accompanied by the high level of stress deducing secondary metabolites (proline, total  
22 flavanoids, phenylpropanoids, and glucosinolides). Moreover, high level of GA<sub>3</sub> produced a  
23 hypersensitive response (HR) in the seedlings. The HR developed cross talks with IAA and  
24 trans-zeatins and triggered higher production of hypersensitive inducing biomolecules. The  
25 other HR co-related biological processes were demonstrated by high phytoalexins level and  
26 high protease activities. Such activities ultimately inhibited the colonization of BIPOL on the  
27 roots of maize seedlings. The products of the genes expressed at high GA<sub>3</sub> also conferred the  
28 deterrence of BIPOL colonization at SD = OD<sub>0.6</sub>. Intriguingly, when we inhibited GA<sub>3</sub>  
29 biosynthesis in the seedlings with aerially sprayed uniconazole, prior to BIPOL treatment, the  
30 BIPOL colonized and subsequently promoted the seedling growth. This low level of GA<sub>3</sub>  
31 after BIPOL treatment checked the high level of secondary metabolites and hypersensitivity  
32 inducing molecules. The results, thus suggested that the aforementioned processes only  
33 happened in the BIPOL at SD (OD<sub>0.6</sub>), whereas the SD at lower levels (OD<sub>0.2</sub> or OD<sub>0.4</sub>)  
34 neither promoted the growth of uniconazole pre-treated seedlings nor produced HR in control  
35 seedlings of maize plant.

36 **Keywords:** Plant-micorbes interaction, hormonal cross talks, growth activity, Uniconazole,  
37 *Zea mays*

38

## 39 **Introduction**

40 Upon the plant microbe interaction, several hypersensitive reactions, including hormonal  
41 biosyntheses and the subsequent signal transduction mechanism are triggered (Kim et al.,  
42 2018). Such signal transduction in host later develops the expression of genes which decide  
43 the fate of microbe interaction with host (Ramirez-Prado et al., 2018). Recently, gibberellins  
44 hypersensitivity accompanied by their signal transduction processes have emerged as a  
45 critical component of plant-microbe interactions (Binenbaum et al., 2018). However, very  
46 little information is available about the cross talk between GAs and other phytohormones in  
47 plant under stress conditions (Zhang et al., 2018). On the other hand, gibberellins signalling  
48 are widely manipulated by the proteolytic activity of DELLA proteins (Xiang et al., 2018).  
49 Most of the interacting plant microbes suppress the proteolysis of DELLA proteins in host  
50 plants by secreting a variety of compounds (Brumos et al., 2018).

51 Hypersensitive response (HR) in plant is triggered upon the interaction of undesired microbe  
52 for host plant (Matić et al., 2016). HR in plant is characterized by the production  
53 hypersensitive inducing molecules such as c-di-GMP, and cAMP (Cadby et al., 2019). Other  
54 signalling molecules such as phosphatidic acid (PA), free or esterified oxo-phytodeinoic acid  
55 (OPDA), and jasmonic acid (JA) are also at the site of HR in host (Hou et al., 2016). These  
56 molecules activates the host defence response against the microbe (Lim et al., 2017).  
57 Accompanied by this, the host plant produces phytoalexins (Suárez et al., 2018) and high  
58 protease activity (Asai and Shirasu, 2015). Primarily, such HR is activated at the response of  
59 high level of phyto-hormone (Großkinsky et al., 2016). In plant, IAA, GA<sub>3</sub> and trans-zeatin  
60 are responsible for the HR (Body et al., 2019).

61 During HR to any stress, the host plant growth is adversely affected which is optimally be  
62 determined by Relative Growth Rate (RGR) (Vasseur et al., 2018) and Net Assimilation Rate  
63 (NAR) (Koch et al., 2019) at different time duration of treatment. In such condition, plant

64 increases the concentration of secondary metabolites in its leaf and roots which combat any  
65 stressing condition (Yang et al., 2018). The commonly determined secondary metabolites in  
66 the plants are proline (Silva et al., 2018), flavonoid contents (Tohge et al., 2018), phenyl  
67 propanoids (PPs) (Hiruma, 2019), and glucosinolates (GLs) (Czerniawski and Bednarek,  
68 2018). Phyto-hormonically in host, HR inducing microbes suppress the E3 ligase  
69 polyubiquitination to inhibit GA<sub>3</sub> from degrading DELLA protein (Li et al., 2019). Most of  
70 the arbuscular fungi (AF) are known to utilize GA<sub>3</sub> signalling in order to produce nodulation in  
71 plant (Mamontova et al., 2019). Pea mutant *cry-s* is known to have high AF colonization due  
72 to reduce level of GA<sub>3</sub> and high DELLA protein activity (McGuinness et al., 2019). Fungal  
73 sporulation specifically needs low GA signalling in host as an optimal environment (Bedini et  
74 al., 2018). The plant host usually discourages the biotroph growth in their tissues by releasing  
75 GA<sub>3</sub> and associated signalling with it (Yimer et al., 2018). It is also worth mentioning that the  
76 surface elicitors of the microbes also contribute to gibberellins hypersensitivity (Mott et al.,  
77 2018).

78 Surface elicitors that are responsible for gibberellins hypersensitivity in host, includes  
79 glycoproteins and Glycolipid (Chaliha et al., 2018). Besides, high level of GA<sub>3</sub> in host plants  
80 also interferes with the other phytohormones (Tijero et al., 2019). GA<sub>3</sub> is known to develop  
81 antagonistic relation with other plant growth hormones, once its level significantly increases  
82 beyond the optimum requirements in the host plants (Fuentes et al., 2019). The production of  
83 higher amounts of GA<sub>3</sub> thus interferes with the growth and development of the host plants  
84 through establishing of cross talks between GA<sub>3</sub> and other phytohormones (Feurtado and  
85 Kermode, 2018).

86 *Bipolaris* is genus of higher fungi frequently found in the plant debris and soil.  
87 (Kurosawa et al., 2018). Although, various species of *Bipolaris* are reported to have growth  
88 promoting agent in plants (Nandhini et al., 2018) but there are some other species which are

89 pathogenic in telomorphic stage, such as *Bipolaris hawaiiensis*, *Bipolaris spicifera*, and  
90 *Bipolaris australiensis* (Nur Ain Izzati et al., 2019). *Bipolaris sorokiniana* is one of the  
91 dubious species of *Bipolaris* which acted as hemibiotroph and cause HR in variety of plant  
92 species (McDonald et al., 2018). Similarly, at several places, this fungus have been reported  
93 as endophytes (Khan et al., 2015). Therefore, there is a wide gap of research to describe the  
94 mode of infection of *B. sorokiniana* (BIPOL). Previous studies suggest that the manipulating  
95 role of the host GA<sub>3</sub>, IAA and TZn is highly unknown during the interaction of BIPOL to  
96 host plant.

97 Presently, we have analysed the GA<sub>3</sub> hypersensitivity at the interaction of BIPOL  
98 with spore densities (Tohge et al.) OD<sub>0.2</sub> OD<sub>0.4</sub> or OD<sub>0.6</sub> and its cross talks with IAA and  
99 cytokinins. Also, it was determined that how GA<sub>3</sub> cross talks with IAA and trans-zeatin can  
100 effect BIPOL colonization in host root (maize seedlings) and the related host growth  
101 responses.

## 102 **MATERIALS AND METHODS**

### 103 **Plant materials**

104 Seeds of *Zea mays* (var. *Hysun-33*) were obtained from BCSS (Bio Care Service Seeds) and  
105 kept at 4 °C for 21 days for vernalisation period (Müller et al., 2017). At the time of  
106 experiment, the seeds were treated with dilute solution of HgCl<sub>2</sub> (0.1%) for 10 seconds and  
107 then surface sterilized with 70 % ethanol (Sen et al., 2013). The sterilized seeds were washed  
108 with autoclaved distilled water to rinse off any surface adsorbent. The sterilized seeds were  
109 then shifted to Petri plate having filter paper moistened with distilled autoclaved water.  
110 Afterwards, the Petri plates were wrapped in an aluminium foil and incubated at 25 °C for 3  
111 days. Germinated seedlings of same vigour were selected and shifted to pots having  
112 standardized Hoagland solution as described (Hassan, 2017). The seedlings were  
113 acclimatized in the Hoagland solution for 3 days and then the seedlings were shifted to four

114 different sets to receive different treatment. The first set of maize seedlings were treated with  
115 2 mL fungal spore in Hoagland solution to grow (B). Leaves of second set of maize seedlings  
116 were sprayed with 2 mL 10 mM yucasin (Y). The third set received both treatment as fungal  
117 inoculation at roots of the seedlings after 12 hours pre-treatment of Yucasin (Y-B). Control  
118 seedlings did not receive any of the above mentioned treatment (C).

### 119 **Preparation of fungal inoculum for infection assay**

120 The culture of previously isolated, identified and preserved BIPOL (Asaf et al., 2019) was  
121 refreshed at 28 °C on PDA. About, 0.02 g of the fungal spores were transferred to a 500 mL  
122 flask containing 250 mL of potato dextrose broth in the flask and then incubated at 25 °C for  
123 5 days in a shaking incubator operated at 150 rpm (Khan et al., 2015). On the 5<sup>th</sup> day, 1 mL  
124 of the inoculum from the spore suspension was taken and transferred to a fresh potato  
125 dextrose broth. The fresh culture broth was kept overnight at 25 °C in a shaking incubator.  
126 Prior to inoculation, the spore was washed by centrifugating at 10<sup>5</sup> xg at 10 °C for 30 min in  
127 sterile distilled water trice (Huttenlocher et al., 2019). Optical density (OD) of the washed  
128 spore's suspension was measured at 600 nm and adjusted to OD<sub>0.2</sub> or OD<sub>0.4</sub> or OD<sub>0.6</sub> with the  
129 help of sterilized distilled water. We used germinated spore to inoculate the plant to  
130 accelerate the colonization potential of *B. sorokiniana* (Selvakumar et al., 2018).

### 131 **Determination of fungal root colonization**

132 Root segments of seedlings of the fungal treatment were kept on a Petri plate containing PDA  
133 media and then incubated at 25 °C. To calculate fungal colonization frequency, the relative  
134 number of the root segments occupied by the fungus was observed.

### 135 **Preparation of Sample for biochemical analyses**

136 For phytochemical analyses, fresh leaves were quickly frozen in liquid nitrogen and ground  
137 to obtain fine powder in a mortar and pestle. Absolute methanol (200 mL) was then added to  
138 the fine powder (2 gm) and the solution was transferred to the soxhlet apparatus for the

139 extraction of phytochemicals (Dhawan and Gupta, 2017). The obtained leaf extract (LE) was  
140 first filtered and the filtrate was concentrated in the rotary evaporatory (Wahyuningsih et al.,  
141 2017). Moreover, root exudates (RE) was obtained from filtered hydroponic culture of the  
142 root seedlings and concentrated in the rotary evaporatory.

### 143 **Secondary metabolite determination**

144 Colorimetric method was used for the evaluation of total flavonoids and proline contents.  
145 Samples (1 mL) of LE and RE were prepared as mentioned above, mixed in 3 % sulfo-  
146 salicylic acid (4 mL) and centrifuged for 5 mins at 6077 rcf. After centrifugation, the 2 mL of  
147 ninhydrin reagent was added to the samples and shaken vigorously. Acid ninhydrin reagent  
148 was prepared by adding 1.25 g of ninhydrin in pure glacial acetic acid (30 mL) and 20 mL of  
149 phosphoric acid (6 M) and mixed. The reaction mixture was heated for 1 hour at 100 °C and  
150 the pellet found was disappeared in toluene (4 mL) (Lee et al., 2018). OD of the samples  
151 were monitored using UV/Vis spectrophotometer (Lambda 1050) at 520 nm. Similarly, for  
152 determination of total flavonoid contents, 0.5 mL of LE and RE samples were added into 10  
153 % potassium acetate (100 µL), 10 % aluminium chloride (100 µL), 70 % ethanol (4.3 mL).  
154 The mixture was incubated at room temperature for 30 minutes and the OD was measured at  
155 450 nm on UV/Vis spectrophotometer (Lambda 1050) (Gil-Ramírez et al., 2016).

156 Phenylpropanoids and glucosinolates were determined using HPLC technique by  
157 taking ferulic acid (Genovese et al., 2018) and indolyl glucosinolates (Aghajanzadeh et al.,  
158 2019) as standards respectively. The samples (RE or LE) first were filtered through a 0.2 µm  
159 membrane filter associated in a syringe filtration. The filtrated sample (20µL) was then  
160 poured into a C18 reverse phase HPLC column and eluted with 75 % methanol (in % 10  
161 acetic acid) for Phenylpropanoids and glucosinolides through an isocratic pump. The eluate  
162 was monitored through a UV detector set at 212 nm and 287 nm for Phenylpropanoids and  
163 glucosinolates respectively (Jeon et al., 2018).

## 164 **Enzymatic activities determination**

165 Oxidase and catalase activities were determined in the LE and RE samples (Röcker et al.,  
166 2016). For the determination of oxidase activity, sample (200  $\mu$ L) was mixed with 1.5 mL of  
167 phosphate buffer (50 mM), 200  $\mu$ L of ascorbic acid (0.5 mM), and 200  $\mu$ L of H<sub>2</sub>O<sub>2</sub> (0.1 mM)  
168 in a cuvette. OD was measured with an interval of 30 seconds at 290 nm. The collected data  
169 was averaged for each sample and expressed in enzyme units per gram of tested sample  
170 ( $\text{Ugm}^{-1}$ ). For calatase activity determination, reaction mixture was prepared by mixing 40  $\mu$ L  
171 sample with 400  $\mu$ L of H<sub>2</sub>O<sub>2</sub> (15 mM) and 2.6 mL of phosphate buffer (50 mM). The OD was  
172 measured at 240 nm for each sample using the same procedure as for oxidase activity  
173 determination (18).

174 Similarly, Cofactor NAD<sup>+</sup> (Nicotinamide adnenine dinucleotide) was determined by  
175 adding 2 mL sample (LE or RE) into 50  $\mu$ L MgCl<sub>2</sub> (500 mM), Tris-HCl Buffer (0.5 mL) and  
176 100  $\mu$ L FADH. Reaction was started by adding 500 mL G6P (500 mM) into reaction mixture.  
177 OD was monitored on 340 through spectrophotometer (Hughes et al., 2015). Cofactor FAD<sup>+</sup>  
178 (Flavin adnenine dinucleotide) was determined by adding 2 mL sample (LE or RE) into  
179 reaction mixture containing 1 mL HEPES (50 mM), 100  $\mu$ L ascorbic acid (250 mM) and 100  
180  $\mu$ L FADH. Reaction was initiated by adding Metolachlor OA (C<sub>15</sub>H<sub>21</sub>NO<sub>4</sub>). Optical density  
181 was monitored at 340 without any incubation through photo-spectrometer (Ceh-Pavia and Lu,  
182 2016).

## 183 **Intracellular determination of c-di-GMP and cAMP level**

184 Freshly taken leaf or root section (2 gm) was homogenised by centrifugation at 5000 g, for 30  
185 min. The cell pellet was suspended in 1 mL extraction buffer (40 % methanol, 0.1 % formic  
186 acid, 40 % acetonitrile, and 19.9 % distilled water) and vortexed for 30 sec. The sample was  
187 incubated for 30 min. after incubation, lysing was done in by using non-contact ultra-  
188 sonication (UCD-200, Belgium) (Jenal et al., 2017). The samples were subjected to HPLC-



189 MS/MS on QTRAP 4500 system (USA) (Jenal et al., 2017). The results was compared with  
190 the standards of the pure c-di-GMP and cAMP levels.

### 191 **Quantification of hypersensitive inducing molecules**

192 Quantification of hypersensitive inducing molecules as pure Oxo-phytodeinoic acid (OPDA),  
193 esterified OPDA, phosphatidic acid (PA) and jasmonic acid (JA). Root or leaf tissues (2 gm)  
194 were taken into glass tube containing 5 mL distilled water and agitated in orbital shaker.  
195 After removing root or leaf tissues, samples were acidified by adding 50  $\mu$ L HCL (1.6 M).  
196 Phase separation was done through mixing ethyl acetate (2 mL) and then dried into nitrogen  
197 gas stream. The samples were then dissolved into methanol (50  $\mu$ L) and subjected to HPLC-  
198 MS/MS on QTRAP 4500 system (USA). The results was compared with the standards of  
199 pure OPDA, esterified OPDA, JA and PA.

### 200 **HPLC-ESI-MS/MS Analyses of phyto-hormones**

201 Hormonal level including IAA (Indole-3-acetic acid), GA<sub>3</sub> (Gibberellin) and Trans-Zeatin  
202 (TZn) in the LE and RE was observed through HPLC-ESI-MS/MS. LE and RE (10 mL)  
203 centrifuged by 6744 rpm for 20 mins. The obtained supernatants were concentrated in  
204 vacuum centrifugation concentrator (Heto-Holten, Denmark) to 5 mL. The concentrated  
205 supernatant was first filtered through 0.22 mm disposable cellulose acetate membrane and  
206 then subsequent determination with by HPLC-ESI -MS/MS. For the analyses through  
207 HPLC-ESI -MS/MS, the aligent 1260 HPLC apparatus was connected with a aligent 6410B  
208 mass spectrometer equipped with Park nitrogen generator (11.0L/ min Nitrogen flow and a  
209 negative mode an electrospray ionization source (4000 V, 45 psi) and). Mobile phase was  
210 made by adding acetonitrile (0.1 % formic acid) into acidic water (0.1 % formic acid) in ratio  
211 of 2:1 at a flow rate of 0.5 mL/min for 40 min. Hormonal analysts (IAA, GA<sub>3</sub>, TZn) were  
212 monitored at 312.9 m/z, 391.6 m/z, and 379.4 m/z respectively. For method validation,  
213 standard solution of IAA, GA<sub>3</sub>, and TZn were flushed into mobile phase on auto sampler.

## 214 **Measurement of Protease Activity**

215 Protease activity in the root or leaf tissues was observed by spectrofluorometric instrument  
216 (FLX800, BioTek) with suc-LLVY-NH-AMC (sigma fluorogenic substrate for general  
217 protease activity) at excitation wavelength 350 nm and emission wavelength 470 nm, Z-LRR-  
218 amino luciferin (sigma fluorogenic substrate for serine protease activity) at excitation  
219 wavelength 370 nm and emission wavelength 495 nm and Caspase-3 Substrate I (sigma  
220 fluorogenic substrate for cysteine protease activity) at excitation wavelength 355 nm and  
221 emission wavelength 485 nm. Reaction mixture was made by adding 50 µg ground sample  
222 (leaf or root) into 220 µL proteolysis buffer (2 mM ATP, 10 mM KCl, 100 mM HEPES-  
223 KOH, 5 MM MgCl<sub>2</sub>, pH adjusted at 7.5). The general protease activity was monitored  
224 through release of amino-methyl-coumarin (AMC), luciferin, and Capase-3 at result of  
225 reaction of sample and substrate at every 2 min and average was obtained.

## 226 **Quantification of Phytoalexins in maize**

227 Phytoalexins commonly found in maize under HR (zealexin A4, kauralexin A4, DIMBOA  
228 ((2,4-dihydroxy-7-methoxy-1,4-benzoxazin-3-one) and HDMBOA (4,7-dimethoxy-2-{[3,4,5-  
229 trihydroxy-6-(hydroxymethyl)oxan-2-yl]oxy}-3,4-dihydro-2H-1,4-benzoxazin-3-one))  
230 (Block et al., 2019) (Yang et al., 2019) were quantified using HPLC (Thermofisher scientific)  
231 which was coupled with MS (UltiMate 3000 HPLC) with a software (Thermo Xcalibur  
232 software 2.10) (Fu et al., 2018). RE or LE (2 mL) was mixed into extraction buffer (10 mL)  
233 made of HCl 1:2:0.002 H<sub>2</sub>O::2-propanol 37 %, (v/v/v) and then vortexed for 25 sec. After  
234 rigorously shaking, first DCM (dichloromethane) was mixed with the extraction buffer in 2:1  
235 ratio (extraction buffer :DCM). Both samples (RE or LE) were centrifuged for 40 minutes at  
236 6077 rcf. Lower phase was taken and transferred with Pasteur pipette to Pyrex glass culture  
237 tubes. The samples were concentrated using N<sub>2</sub> flow (10 bar) and later heated at 42 °C. The

238 dried samples (2 mg) was then mixed in 2 mL of methanol in water (95.9 %). The samples  
239 were filtered by spin-X centrifuge tube at 10,000 x g.

240 The samples (phytoalexins extracted) were then exposed to HPLC coupled MS by  
241 injecting 20 µl sample into HPLC (Ultimate 3000) armed with a Reverse-phase column  
242 (Acclaim120 C18) at 35 °C with flow rate 0.2 mL/min. The mobile phase used was prepared  
243 by adding 0.1% formic acid in water (solvent A), and 0.1% formic acid with methanol  
244 (solvent B). Solvent gradients were collected at different time duration. The elute was  
245 deducted at 1 hour (retention time). The levels of phytoalexins was then measured by  
246 electrospraying the HPLC effluent into the mass spectrometer (Orbitrap XL) with R =  
247 30,000. Measurements was collected at mass range (m/z 110-460) with the settings (+ive  
248 ionization mode, 4.7 kV, 280 °C capillary temperature, 35 au sheath gas flow rate and 28 au  
249 Aux Ga flow rate). For method validation, known quantities of the standard phytoalexins to  
250 RE and LE were analyzed using HPLC coupled MS (Ding et al., 2018).

### 251 **Electrolytic leakage**

252 Electrolytic leakage (EL) was measured as described (Orrego et al., 2019). Briefly, 0.3 g of  
253 leaf from every individual plant was washed with deionized water and then placed in 15 mL  
254 of falcon tube containing 15 mL of deionized water. The samples were incubated for 2 hours  
255 at 25 °C (13) and the electrolytic conductivity of the sample ( $L_1$ ) was recorded. Samples were  
256 then autoclaved at 120 °C for 20 minutes, cooled down to 25 °C and the EC ( $L_2$ ) was  
257 measured again.

258 The final read was obtained using the formula:

$$EL (\%) = \frac{L_1}{L_2} \times 100$$

259 **Determination of marker genes involved in HR at GA<sub>3</sub> cell signaling perception and**  
260 **repression**

261 Data available for GA<sub>3</sub> cell signaling perception and repression under host-microbe  
262 interaction at Expression Angler 2016 (<http://bar.utoronto.ca/ExpressionAngler/>) of BAR  
263 were extracted using the co-related gene expression with r-cut off range from 0.7 to 1.0 and -  
264 0.1 to -0.7 (Holland and Jez, 2018). The reference microbes used to extract the data were  
265 *Pseudomonas syringae* vs tomato DC3000, a bacterial hemibiotroph (Narusaka and Narusaka,  
266 2017), *Botrytis cinerea* a fungal necrotroph (Petrasch et al., 2019), *Phytophthora infestans*, a  
267 fungal hemibiotroph (Zuluaga et al., 2016) and *Erysiphe orontii*, a fungal biotroph (Bheri et  
268 al., 2019) to obtain the universal marker genes at GA<sub>3</sub> cell signaling perception and  
269 repression in the above mentioned r-cut off range. Using yED Graph Editor, raw data was  
270 formatted and visualized (Reissmann and Muddukrishna, 2018). In such visualization, red  
271 balls indicated the upregulating genes with the subject gene (*GIDI* or *RGRI*) and blue balls  
272 represented downregulating gene. The role of each co-expressed genes significant at our  
273 subject study was determined on TAIR (The *Arabidopsis* Information Resource)  
274 ([www.arabidopsis.org](http://www.arabidopsis.org)) (Consortium et al., 2019). Homologues of 9 marker genes expressed  
275 in *Arabidopsis thaliana* were obtained in maize seedling using maize genome database  
276 ([www.maizegdb.org](http://www.maizegdb.org)) (Portwood et al., 2018). The expression of such 9 genes were analyzed  
277 using qRT-PCR technique in the root sample of 11 days old seedlings of maize.

#### 278 **Extraction of RNA and subsequent qRT-PCR analysis**

279 Spectrum Plant Total RNA Kit (Sigma Aldrich) was added into the host root sample for RNA  
280 extraction. DNase I was also mixed to remove any genomic DNA in the sample during RNA  
281 extraction (Yin et al., 2016). Primers (Table S1) of oligo (dT)s with Super-Script III First  
282 Strand Synthesis SuperMix (Invitrogen) with s added to generate cDNA library (Hoegge et al.,  
283 2017). The qRT-PCR invitrogen 1x SYBR Green I was done in a CFX96 Real time PCR  
284 (Bio-Rad detection system) (Amaral et al., 2017). In order to normalise the expression level  
285 of target genes, expression of housekeeping genes (*DPP9*) was compared (Amaral et al.,

286 2017). The primers for genes (Table S1) were designed using online *Oli2go* (  
 287 <http://oli2go.ait.ac.at/>) on desired temperature and primer length (Hendling et al., 2018).

288 **Table S1:** List of primers used for the expression of 9 markers gene in maize seedlings

S. No.	Genes in <i>A. thaliana</i>	Homologue of Maize Gene (ID)	Primers
1.	<i>GID1</i>	<i>Zm00001d010308</i>	Forward TTCTTCTGTTGGGATGCGCC Reversed GGATTGAGCCCAAAGGGGAA
2.	<i>RGA1</i>	<i>Zm00001d041362</i>	Forward GTTGCTTGAGCCTTGTCAGC Reversed AACCTGGCAGCGATGCTATT
3.	<i>WII2</i>	<i>Zm00001d002065</i>	Forward GCAACCTGGGTGGTTCGATTA Reversed ACATTGTGCGCGAAAGCAAA
4.	<i>TRX5</i>	<i>Zm00001d002690</i>	Forward ACTCCTTCCAGAACCACCTCC Reversed GGAAGGCAAGGCTGATACTGT
5.	<i>PTF1</i>	<i>Zm00001d045046</i>	Forward CAGACTGAGGTGCCAAACCT Reversed AACTGGCATCAGGCAGAGTC
6.	<i>DPMS2</i>	<i>Zm00001d034682</i>	Forward GCTGACTAGCAGAGGTGCAA Reversed AGCACGGTGCATACCTCTTC
7.	<i>TAT3</i>	<i>Zm00001d053107</i>	Forward CTTCCAGGTAGTGCACAGCA Reversed AGAAGGAGCGATACCTGGCA
8.	<i>WRKY15</i>	<i>Zm00001d036542</i>	Forward GCTAGGTCTGTGCGTGTCT Reversed GCTCCACGAGTTCTTCACGA
9.	<i>ga20ox2</i>	<i>Zm00001d007894</i>	Forward CAACATTGGCGACACCTTCG Reversed TCTGCGTGAACCTCGAGGAAC

289

290

## 291 RESULTS

### 292 Growth promotion under BIPOL inoculation and GA<sub>3</sub> inhibition

293 Growth promotion of plants under endophytic interaction is evaluated by RGR (Vasseur et  
294 al., 2018) and NAR (Koch et al., 2019). We recorded RGR and NAR of the maize seedlings  
295 under interaction of BIPOL at host root with SD (OD<sub>0.2</sub> or OD<sub>0.4</sub> or OD<sub>0.6</sub>) at high or low host  
296 GA<sub>3</sub> level. GA<sub>3</sub> in host plant host was inhibited by pre-treated the host with uniconazole at  
297 leaf (**Figure 2A-2B**). Recorded data revealed that growth was promoted once GA<sub>3</sub> was  
298 inhibited after BIPOL inoculation at SD (OD<sub>0.6</sub>) (**Figure 1C & 1F**). However, the growth  
299 was found to be very low at uniconazole treatment till 72 hour, while later restored (**Figure**  
300 **1A & 1D**). Surprisingly, when we challenged the host with BIPOL alone at SD (OD<sub>0.6</sub>), the  
301 growth of seedlings became highly compromised (**Figure 1B & 1E**). Moreover, when we  
302 treated the seedlings with BIPOL SD (OD<sub>0.2</sub> or OD<sub>0.4</sub>), the seedlings did not respond to both  
303 SDs (**Figure S1A & S1C**). Similarly, the both SDs also could not promote growth at  
304 uniconazole pre-treated seedlings when maize seedlings were at stress till 72 h (**Figure S1B-**  
305 **S1D**).

306 Cell wall integrity is very essential for the host under growth promoting condition  
307 (Mirabet et al., 2018). We determined the integrity by Electrolytic leakage (EL) as high EL  
308 value refers to host cell wall stability (Mihailova et al., 2018). As expected, EL was low in  
309 U-B seedlings at SD (OD<sub>0.6</sub>) (**Figure 1I**). However, the uniconazole pre-treated seedlings of  
310 maize had high EL till 72 h which later became same as control (**Figure 1G**). As opposed,  
311 EL was very high in BIPOL treated seedlings of maize at SD (OD<sub>0.6</sub>) (**Figure 1H**). Similarly,  
312 there found no change observed in EL at SD (OD<sub>0.2</sub> or OD<sub>0.4</sub>) in control or with pre-treatment  
313 of uniconazole to maize seedlings (**Figure S1E-S1F**).

### 314 Hormonal cross talks under BIPOL interaction with host

315 The interacting microbe alters the certain specific host hormonal level to successfully  
316 colonize in the host tissues (Chagas et al., 2018). Such altered hormone level produced a  
317 cross talk with other hormones which in turn produce a HR in host (Bürger and Chory, 2019).  
318 In case of BIPOL interaction with host, we observed essential hormonal cross talks of GA<sub>3</sub>,  
319 IAA and TZn levels treated seedlings. When we inhibited GA<sub>3</sub> level in host by treating with  
320 uniconazole at leaf till 72 hr, the level of IAA and TZn was not affected (**Figure 2A-2B, 2F-**  
321 **2G, 2K-2L**). However, after 72 h, the U seedlings restored GA<sub>3</sub> (**Figure 2C-2E**). However,  
322 the host treated with BIPOL SD (OD<sub>0.6</sub>) triggered high GA<sub>3</sub> level (**Figure 2A-2E**).  
323 Meanwhile the IAA and TZn was observed very low (**Figure 2F-2O**). Interestingly, in U-B  
324 seedlings, the level of IAA and TZn remained high with low GA<sub>3</sub> level during all treatment  
325 hours (**Figure 2A-2O**). Additionally, the SD (OD<sub>0.2</sub> or OD<sub>0.4</sub>) could not triggered high GA<sub>3</sub> in  
326 host thus the level of IAA and TZn was optimal as control (**Figure S2A-S2F**). Similarly, in  
327 GA<sub>3</sub> inhibited seedlings (U seedlings), the SD (OD<sub>0.2</sub> or OD<sub>0.4</sub>) also could not restore GA<sub>3</sub>  
328 (**Figure S2A-S2F**).

### 329 **Secondary metabolites in host under BIPOL interaction**

330 Secondary metabolites are produced in plants to avoid deleterious effect of biotic and abiotic  
331 stresses at the expense of plant growth and development (Yang et al., 2018). In plants,  
332 flavonoids (Tohge et al., 2018) and proline (Silva et al., 2018) are the two important group of  
333 secondary metabolites which are induced in plant under stress condition. We determined total  
334 flavonoid content and proline in LE and RE of maize through spectrophotometry technique  
335 (Zhou et al., 2018). The results showed that LE and RE had low contents of the secondary  
336 metabolites (total flavonoids and proline) in growth promoted U-B seedlings till 120h at SD  
337 (OD<sub>0.6</sub>) (**Figure 3A-3J**). Conversely, the concentration of total flavonoids and proline in the  
338 growth compromised BIPOL seedlings (OD<sub>0.6</sub>) was high during the same duration (**Figure**  
339 **3A-3J**). However, in uniconazole treated seedlings, the metabolites were initially increased

340 till 72 h (**Figure 3A-3C & 3F-3G**), followed by a significant drop in the later hours (**Figure**  
341 **3D-3E & 3I-3J**). Additionally, SD (OD<sub>0.2</sub> or OD<sub>0.4</sub>) could not elicit the production of total  
342 flavonoid contents and proline (**Figure S3A-S3B & 3E-3F**). Similarly, these SDs also could  
343 not reduce the two group of secondary metabolites in 72 h in pre-treated U seedlings (**Figure**  
344 **S3C-S3D & 3G-3H**).

345 We also quantified phenylpropanoids and glucosinolates in the treatment condition  
346 through GC/MS technique by taking ferulic acid and indolyl glucosinolate as internal  
347 standards respectively. Phenylpropanoids and glucosinolates are the group of secondary  
348 metabolites produced in plants upon the exposure to various biotic or abiotic stresses (Bhatla,  
349 2018). These compounds aid the plant to cope with the environmental stresses (Obata, 2019).  
350 As expected from **Figure 3K-3T**, uniconazole treatment triggered high amount of  
351 phenylpropanoids and Glucosinolates till 72 h while later became less. BIPOL treatment SD  
352 (OD<sub>0.6</sub>) induced highest amount of these two compounds (**Figure 3K-3T**). Interestingly, the  
353 U-B seedlings SD (OD<sub>0.6</sub>) triggered low amount of these two groups of compounds (**Figure**  
354 **3K-3T**). However, the amount of these two groups of compounds were same as control in SD  
355 (OD<sub>0.2</sub> or OD<sub>0.4</sub>) (**Figure S3I-S3J & S3M-S3N**). Similarly, at UNI treatment, the both SD  
356 (OD<sub>0.2</sub> or OD<sub>0.4</sub>) could not lowered the amount of phenylpropanoids and Glucosinolates  
357 (**Figure S3G-S3L & S3O-S3P**).

### 358 **Enzymatic activity under BIPOL inoculation**

359 We determined different enzymatic activities in the LE and RE maize seedlings which are  
360 operated under various stress condition (Luis et al., 2018). Two well-known enzymatic  
361 activity in host is catalase and oxidase enzymatic activities (Zheng et al., 2018). Catalase  
362 activity is severally decreased upon the plant exposure to biotic or abiotic stresses (Farooq et  
363 al., 2019). The catalase activity was low in the uniconazole treated seedlings of maize till 72  
364 hours which later decreased (**Figure 4A-4E**). In U-B seedlings of maize at SD OD<sub>0.6</sub>, the



365 catalase activity remained high (**Figure 4A-4E**). However, in BIPOL treated seedlings of  
366 maize SD (OD<sub>0.6</sub>), the catalase activity was very low till 120 hours (**Figure 4A-4E**).  
367 Additionally, BIPOL inoculation SD (OD<sub>0.2</sub> or OD<sub>0.4</sub>) could not increase catalase activity  
368 (**Figure S3A-S3B**). Similarly, the both SD (OD<sub>0.2</sub> or OD<sub>0.4</sub>) also could not decreased catalase  
369 activity in uniconazole treated seedlings of maize till 72 hours (**Figure S3C-S3D**).

370 Oxidase activity is induced upon the elevated stress condition on plant (Joshi et al.,  
371 2018). As expected, uniconazole treatment to maize seedlings increased oxidase activity till  
372 72 hour which later became normal as control. As opposed to this, the oxidase activity was  
373 low in U-B seedlings of maize at SD (OD<sub>0.6</sub>) (**Figure 4A-4E**). Interestingly, the BIPOL  
374 inoculation SD (OD<sub>0.6</sub>) also increased oxidase activity till 120 hours in maize seedlings  
375 (**Figure 4A-4E**). Additionally, the BIPOL inoculation at SD (OD<sub>0.2</sub> or OD<sub>0.4</sub>) could not  
376 induced oxidase activity (**Figure S4E-S4F**). Similarly, both SD (OD<sub>0.2</sub> or OD<sub>0.4</sub>) also could  
377 not reduce oxidase activity in uniconazole treated seedlings of maize (**Figure S4E-S4F**).

378 During stress condition on plant, certain enzymatic co-factors shot up in the leaf and  
379 also exuded from the plant roots in a growth medium (Speijer, 2019). We determined the  
380 reduction and induction of two major sample co-factors (NAD<sup>+</sup>, FAD<sup>+</sup>) involved in this  
381 process in percent through spectrophotometric technique. As indicated from **Figure 4K-4T**,  
382 the co-factors were highly induced under uniconazole treatment in maize seedling till 72 hour  
383 which later decreased to control. BIPOL inoculation SD (OD<sub>0.6</sub>) triggered high production of  
384 these factors till 120 hours. Conversely, the U-B treatment SD (OD<sub>0.6</sub>) reduced the  
385 concentration of co-factors (**Figure 4K-4T**). The concentration of these enzymatic co-factors  
386 under BIPOL inoculation (OD<sub>0.2</sub> or OD<sub>0.4</sub>) was same as control (**Figure S4I-S4J & S4M-**  
387 **S4N**). Similarly, both SDs also could not reduce the elevated level of enzymatic co-factors in  
388 U seedlings of maize (**Figure S3K-S3L & S3O-S3P**).

389 **Hypersensitive inducing biomolecules under BIPOL inoculation**

390 Certain undesired microbe interaction with plant host produced hypersensitive response  
391 which can be determined by the production of hypersensitive inducing molecules in plants  
392 (Terrón-Camero et al., 2018). We quantified two intracellular signalling molecules for  
393 inducing HR (c-di-GMP (Terrón-Camero et al., 2018) and cAMP level (Almblad et al., 2019)  
394 and four metabolites (phosphatidic acid (PA) pure Oxo-phytodeinoic acid (OPDA), esterified  
395 OPDA, and Jasmonic acid (JA) in maize seedlings through GC/MS technique (Genva et al.,  
396 2019). Result deducted that under uniconazole treatment, the concentration of these  
397 hypersensitive molecules was same as control (**Figure 5A-5J & 6A-6T**). Contrary, in BIPOL  
398 inoculation SD ( $OD_{0.6}$ ), the concentration shot up and reached at their peaks. However, in U-  
399 B seedlings of maize the concentration remained very low (**Figure 5A-5J & 6A-6T**).  
400 Similarly, there occurred no change in the concentration of these molecules under BIPOL  
401 inoculation SD ( $OD_{0.2}$  or  $OD_{0.4}$ ) in pre-treated uniconazole seedlings of maize or without its  
402 pre-treatment (**Figure S5A-S5L**).

403 In dying cell, the protease activity is accelerated to increase auto-digestion of the  
404 organelles in the host cell (Srikantam and Arumugam, 2019). We determined four sample  
405 protease activities (serine protease activity, cysteine proteases, and universal protease  
406 activity) in the maize seedlings under the treatment using fluorescent spectrophotometer.  
407 Results deducted from **Figure 7A-7O** that uniconazole treatment could not cause any protease  
408 activity in the maize seedlings. However, the BIPOL treatment SD ( $OD_{0.6}$ ) triggered high  
409 protease activity. As opposed, the U-B seedlings of maize SD ( $OD_{0.6}$ ) had lowered protease  
410 activity (**Figure 7A-7O**). In addition to this, SD ( $OD_{0.2}$  or  $OD_{0.4}$ ) could not high trigger  
411 protease activity. Similarly, the BIPOL inoculation SD ( $OD_{0.2}$  or  $OD_{0.4}$ ) also could not  
412 produce high protease activity in uniconazole pre-treatment to the maize seedlings (**Figure**  
413 **S5M-S5R**).

414           Upon the initiation of HR in host plant, there occurred cell death mediated by high  
415 amount of phytoalexins in the dying cell (Pitsili et al., 2019). We inspected four sample  
416 phytoalexins commonly found (zealexin A4, kauralexin A4, DIMBOA and HDMBOA) in  
417 maize seedlings (Block et al., 2019) (Yang et al., 2019). As shown in **Figure 8A-8T**, the  
418 concentration of these four phytoalexins remained unchanged in uniconazole treatment to  
419 maize seedlings. Contrary, in BIPOL inoculation SD (OD<sub>0.6</sub>), these occurred high amount of  
420 phytoalexins (**Figure 8A-8T**). In opposed, the sample phytoalexins were noted extremely low  
421 in U-B seedling SD (OD<sub>0.6</sub>). However, in BIPOL inoculation SD (OD<sub>0.2</sub> or OD<sub>0.4</sub>), there  
422 occurred no changed with or without uniconazole treatment to maize seedlings (**Figure S5S-**  
423 **S5X**).

#### 424 **Interfering activity of GA<sub>3</sub> signalling under BIPOL inoculation**

425 We observed the interfering activity of GA<sub>3</sub> cell signal perception and cell signal repression  
426 using co-expression data of GA<sub>3</sub> perception and repression during host-microbe interaction  
427 (**Figure 9A**). The description of the genes were extracted from online Arabidopsis database  
428 available (*TAIR* [www.arabidopsis.org](http://www.arabidopsis.org)). The principle genes included in this case were *WII2*  
429 and *TRX5*. The product of *WII2* and *TRX5* increased the redox potential in the host cell, thus  
430 discouraged the microbial interaction. Similarly, the co-expression of *SNF7*, *EDA16*, *ALA3*  
431 and *PTF1* decreased the vacuolar transportation in the host cell to reduce fungal colonization  
432 on plant tissues. Moreover, in the same manner other cell stabilizing activities such electron  
433 transfer activity, cell apoptosis and modification of sugar molecules to form microbe resistant  
434 biomolecules were also induced by *SAG14*, *RSW10*, *PEP12* and *ADT5* expression (**Figure**  
435 **9A**).

436 Additionally, the co-expression of upregulated DELLA (*RGAI*) determined the high  
437 expression of *DPMS2*, whose product eliminated the oxidative burst to facilitate microbe  
438 interaction (Figure 2b). Similarly, the products of *TAT3*, *SPE3* and *LOL3* commenced the

439 aminotransferase like enzymatic activity to aid in microbe colonization with the host. Other  
440 transcriptional facilitating processes as *WRKY15*, *RABA1*, and *ERD2* for cytoplasmic  
441 streaming to promote the microbe interaction were also upregulated (**Figure 9B**).

442 We selected the 9 marker genes and analyzed its expression during qRT-PCR in 11 days old  
443 maize seedling under treatments. Results deducted from qRT-PCR indicated that expression  
444 of *WII2* (*Zm00001d002065*), *TRX5* (*Zm00001d002690*) and *PTF1* (*Zm00001d045046*) was  
445 highly reduced at U-B seedlings, while the same were upregulated at BIPOL treatment to  
446 maize seedlings (**Figure 10A-10E**). No significance difference was found in uniconazole  
447 treated seedlings of maize compared to control (**Figure 10A-10E**). As opposed to these  
448 expressions, the expression of *DPMS2* (*Zm00001d034682*), *TAT3* (*Zm00001d053107*) and  
449 *WRKY15* (*Zm00001d036542*) was high at U-B seedlings while the same was low at BIPOL  
450 treatment to maize seedlings (**Figure 10F-10J**). No significance difference was found in  
451 uniconazole treatment compared to control (**Figure 10F-10J**).

452 However, the expression of *GID1* (*Zm00001d010308*), *RGA1* (*Zm00001d041362*) and  
453 *ga20ox2* (*Zm00001d007894*) was remained unaffected in uniconazole treatment to maize  
454 seedlings (**Figure 10K-10O**). As opposed, the expression of *GID1* (*Zm00001d010308*) and  
455 *ga20ox2* (*Zm00001d007894*) was very high while *RGA1* (*Zm00001d041362*) was low in  
456 BIPOL treatment (**Figure 10K-10O**). The U-B seedlings of maize followed the exact  
457 opposite trend in the expression of these three genes compared to BIPOL treatment as the  
458 expression of *GID1* (*Zm00001d010308*) and *ga20ox2* (*Zm00001d007894*) was very low  
459 while the expression of *RGA1* (*Zm00001d041362*) was high (**Figure 10K-10O**).

#### 460 **Root colonization of BIPOL under high GA<sub>3</sub> concentration**

461 Fungal colonization was noted very low for BIPOL treated seedlings at SD (OD<sub>0.6</sub>), whereas  
462 it was relatively high in U-B seedlings compared to control seedlings of maize at SD (OD<sub>0.6</sub>)

463 (Figure 11A). However, there was found no change in percent colonization of BIPOL at SD

464 ( $OD_{0.2}$  or  $OD_{0.4}$ ) in both BIPOL and U-B treated seedlings of maize (Figure 11B).

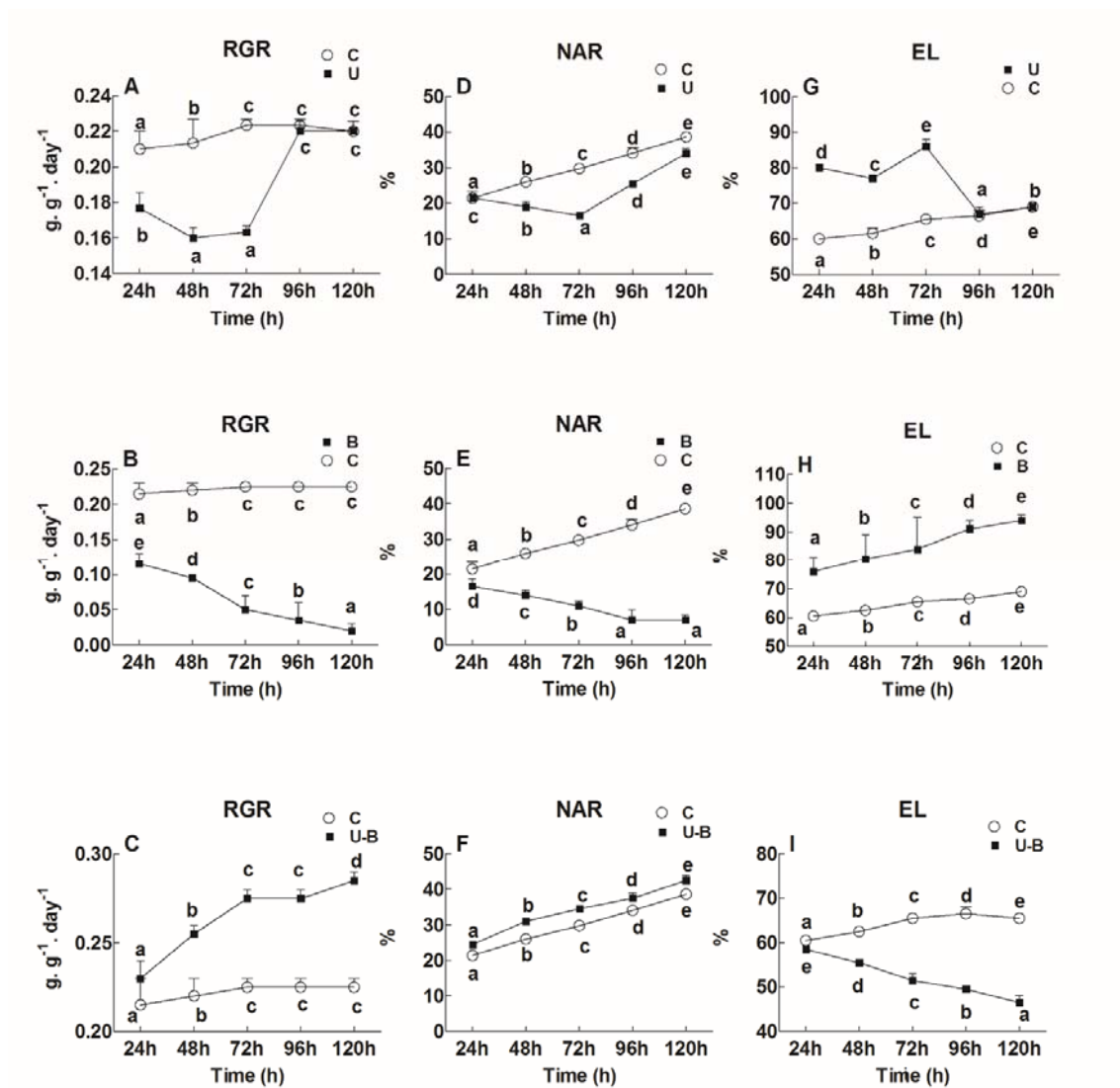
465

466

467

468

469



470

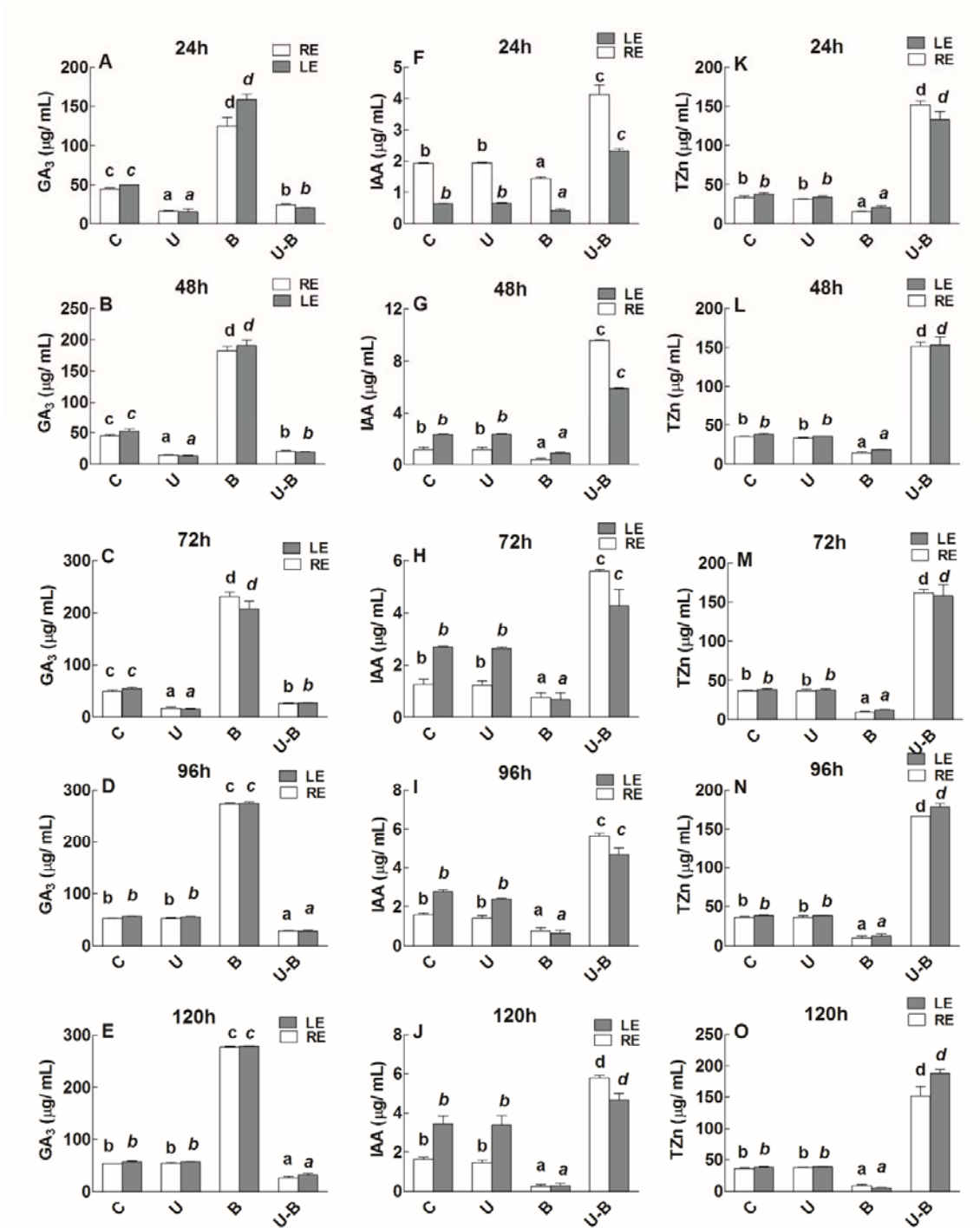
471 **Figure 1**

472 Determination of RGR (relative growth rate), NAR (net assimilation rate), and EC  
473 (electrolytic content leakage) in the 11 days old maize seedlings exposed to different  
474 treatments including C (control), U (Uniconazole), B (BIPOL), U-B (Uniconazole-BIPOL) at  
475 spore density 0.6 for the different time duration. Ducan's test was performed and different  
476 alphabetic letters shows the significant difference. Experiment was repeated at least three  
477 time independently.

478

479

480



481

482 **Figure: 2**

483 Determination of GA<sub>3</sub> (gibberellins), TZn (trans-zeatin), and IAA (indole-3-acetic acid) in  
 484 the LE (leaf extracts) and RE (root exudates) of 11 days old maize seedlings exposed to  
 485 different treatments including C (control); U (Uniconazole), B (BIPOL), U-B (Uniconazole-

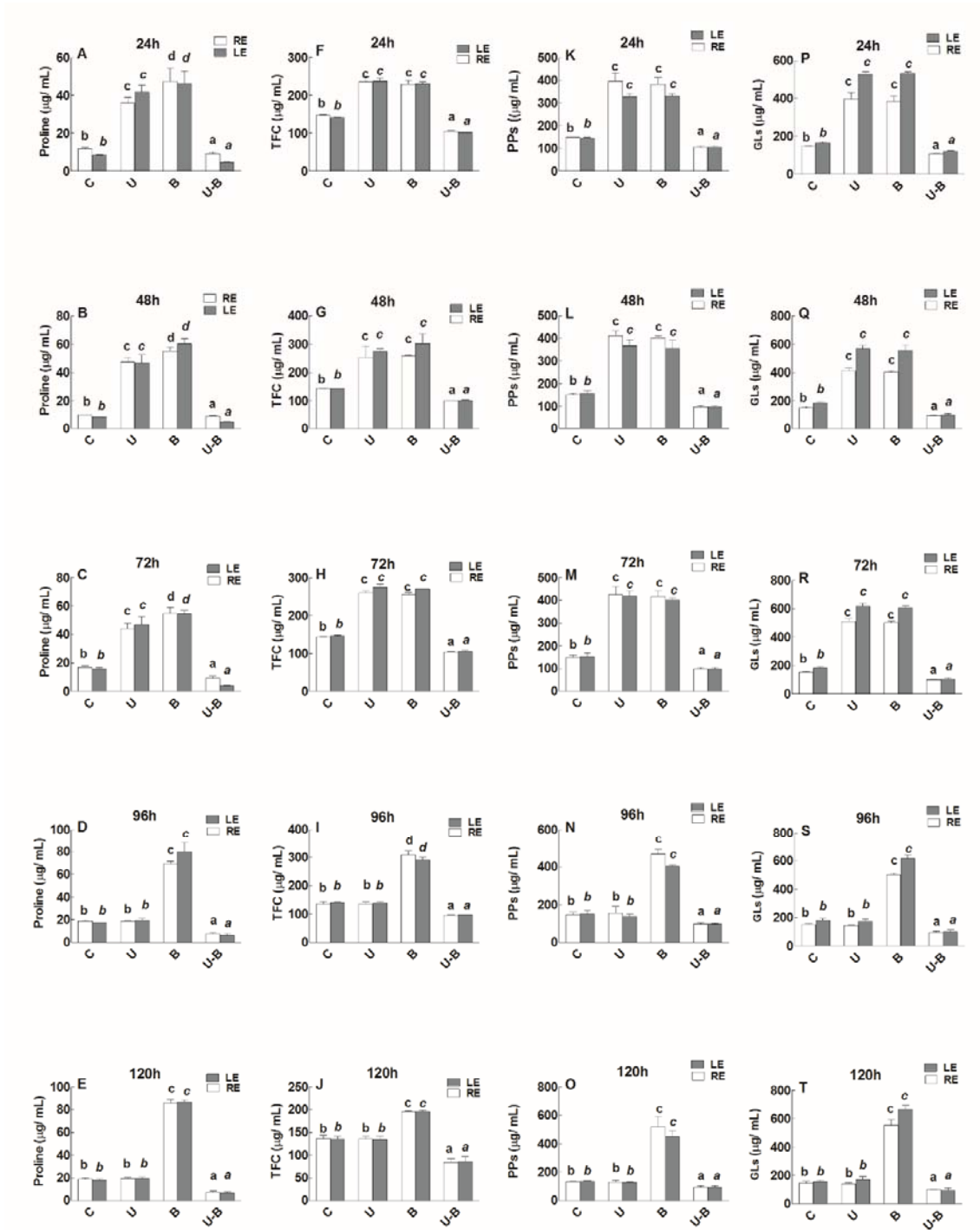
486 BIPOL) for the different time duration. Duncan's test was performed and different alphabetic  
487 letters shows the significant difference. Experiment was repeated at least three time  
488 independently.

489

490

491





492

493 **Figure 3**

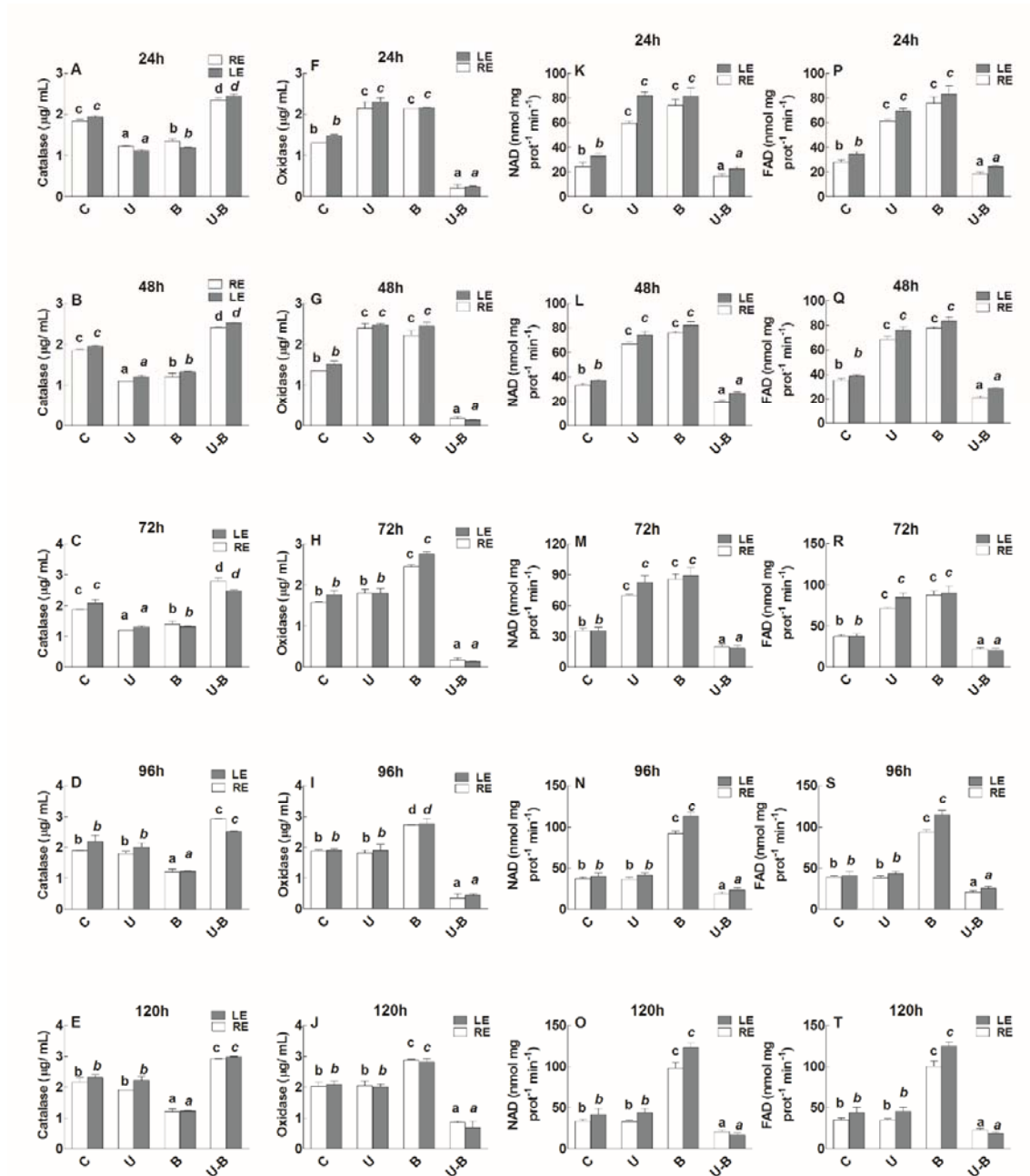
494 Quantification of Proline, TFC (total flavonoid content), PPs (phenylpropanoids) and GLs

495 (Glucosynaloids) in the 11 days old maize seedlings exposed to different treatments

496 including C (control), U (Uniconazole), B (BIPOL), U-B (Uniconazole-BIPOL) at spore

497 density 0.6 for the different time duration. Duncan's test was performed and different  
 498 alphabetic letters shows the significant difference. Experiment was repeated at least three  
 499 time independently.

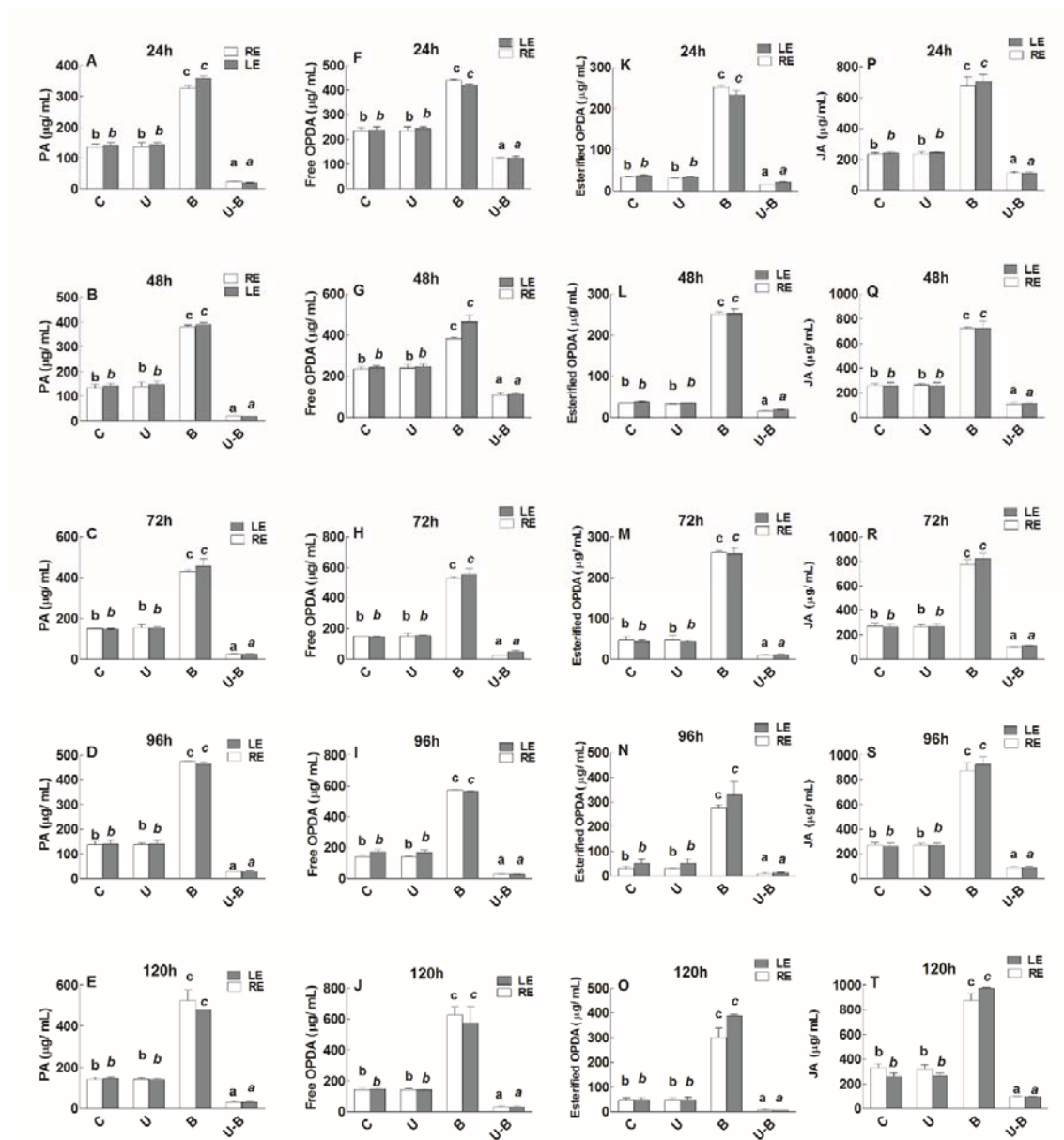
500



501

502 **Figure 4**

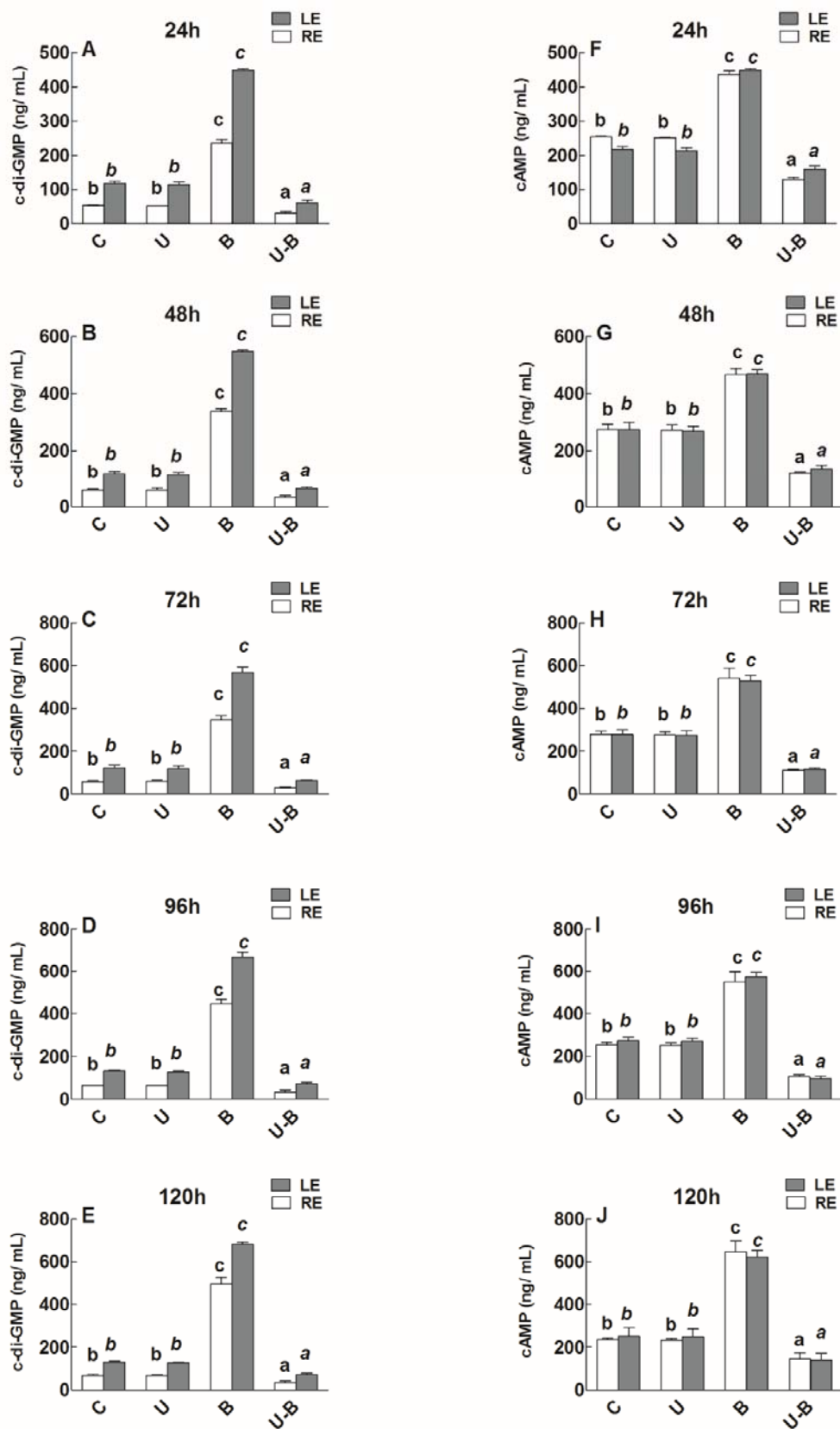
503 Determination of Oxidase, Catalase enzymatic activities, NAD<sup>+</sup> (cofactor) and FAD<sup>+</sup>  
 504 (cofactor) in the 11 days old maize seedlings exposed to different treatments including C  
 505 (control), U (Uniconizole), B (BIPOL), U-B (Uniconizole-BIPOL) at spore density 0.6 for  
 506 the different time duration. Ducan's test was performed and different alphabetic letters shows  
 507 the significant difference. Experiment was repeated at least three time independently.  
 508



509

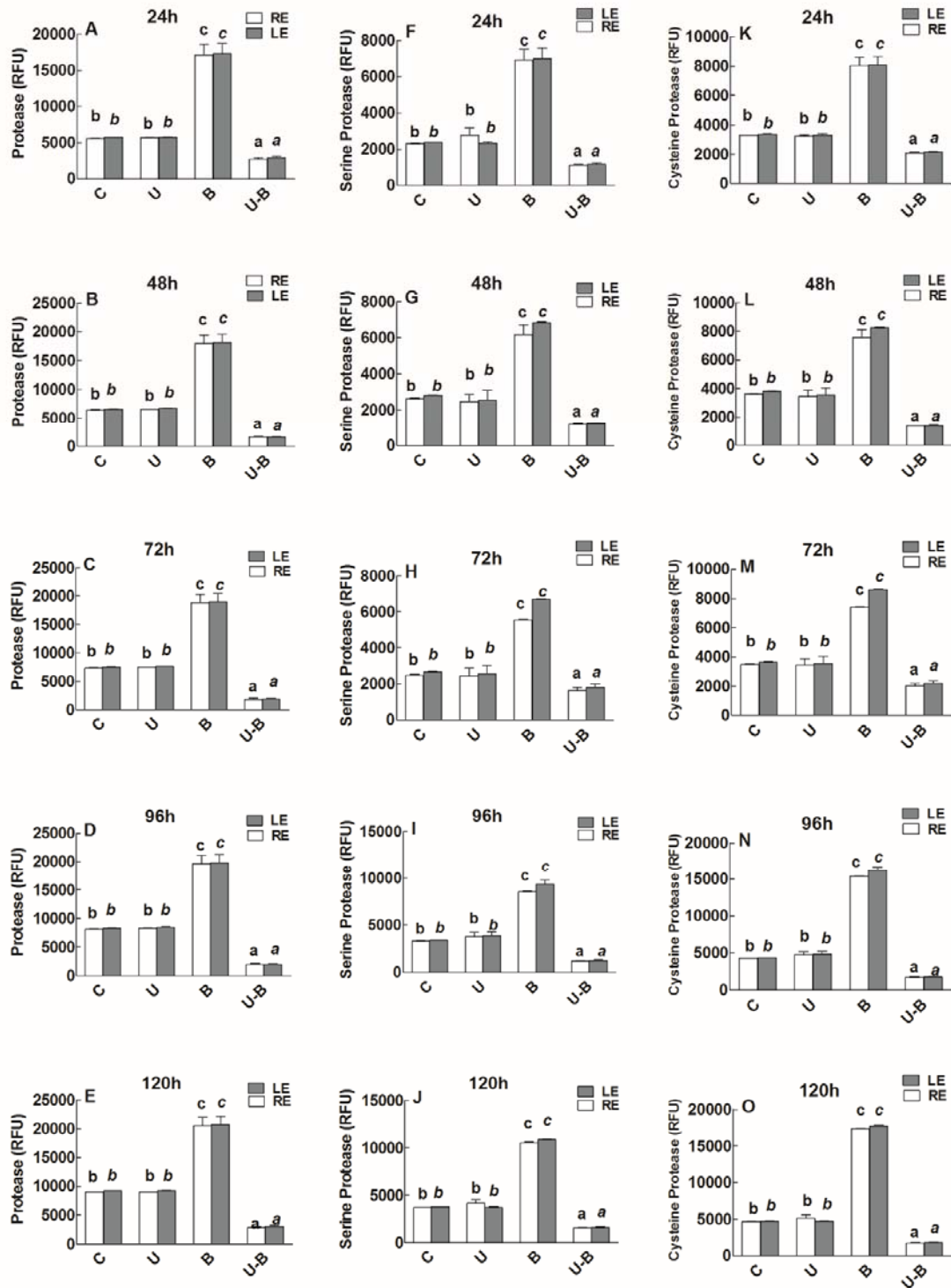
510 **Figure 5**

511 Determination of phosphatidic acid (PA) pure Oxo-phytodeinoic acid (OPDA), esterified  
512 OPDA, and Jasmonic acid (JA) in the 11 days old maize seedlings exposed to different  
513 treatments including C (control), U (Uniconazole), B (BIPOL), U-B (Uniconazole-BIPOL) at  
514 spore density 0.6 for the different time duration. Ducan's test was performed and different  
515 alphabetic letters shows the significant difference. Experiment was repeated at least three  
516 time independently.



518 **Figure 6**

519 Quantification of c-di-GMP (3',5'-cyclic diguanylic acid) and cAMP (3',5'-cyclic adenosine  
520 monophosphate) in the 11 days old maize seedlings exposed to different treatments including  
521 C (control), U (Uniconazole), B (BIPOL), U-B (Uniconazole-BIPOL) at spore density 0.6 for  
522 the different time duration. Ducan's test was performed and different alphabetic letters shows  
523 the significant difference. Experiment was repeated at least three time independently.



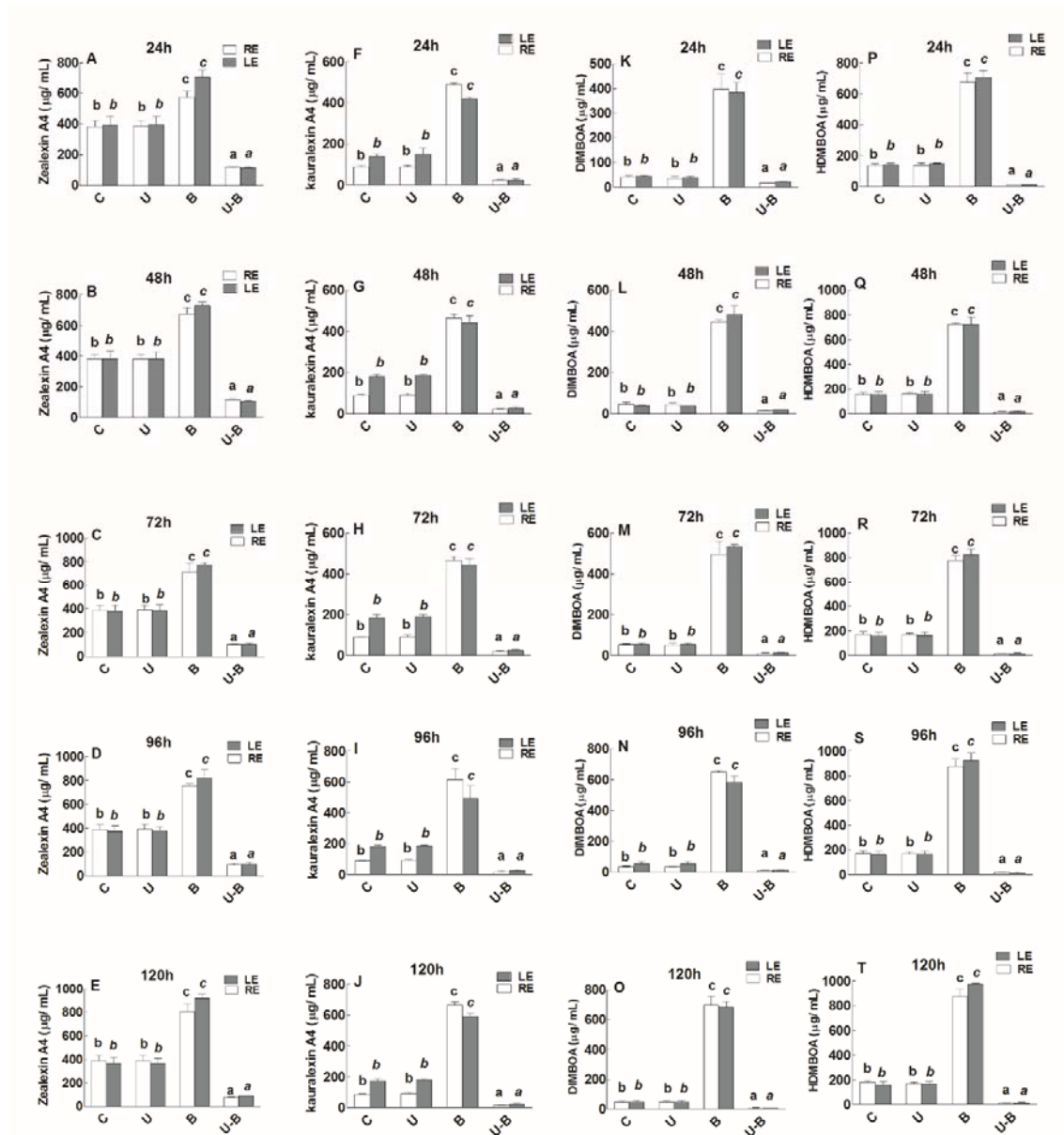
524

525 **Figure 7**

526 Quantification of Universal protease activity, serine protease activity and cysteine protease

527 activity in the 11 days old maize seedlings exposed to different treatments including C

528 (control), U (Uniconizole), B (BIPOL), U-B (Uniconizole-BIPOL) at spore density 0.6 for  
 529 the different time duration. Duncan's test was performed and different alphabetic letters shows  
 530 the significant difference. Experiment was repeated at least three time independently.  
 531



532

533 **Figure 8**

534 Quantification of commonly found phytoalexins in maize (Zeaxelins A4, kauralexin A4,  
 535 DIMBOA and HDMBOA) in the 11 days old maize seedlings exposed to different treatments



536 including C (control), U (Uniconazole), B (BIPOL), U-B (Uniconazole-BIPOL) at spore  
537 density 0.6 for the different time duration. Duncan's test was performed and different  
538 alphabetic letters shows the significant difference. Experiment was repeated at least three  
539 time independently.

540

541

542

543

544

545

546

547

548

549

550

551

552

553

554

555

556

557

558

559

560

561

562

563

564

565

566

567

568

569

570

571

572

573

574

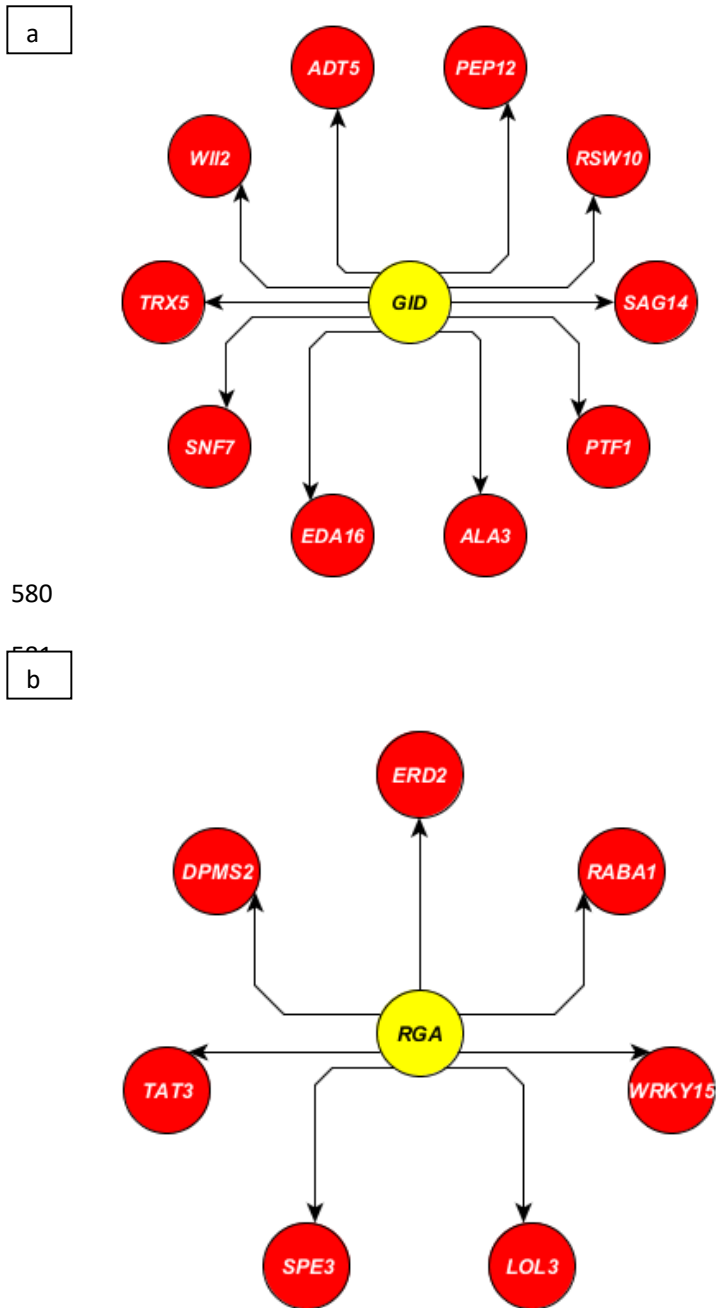
575

576

577

578

579



583

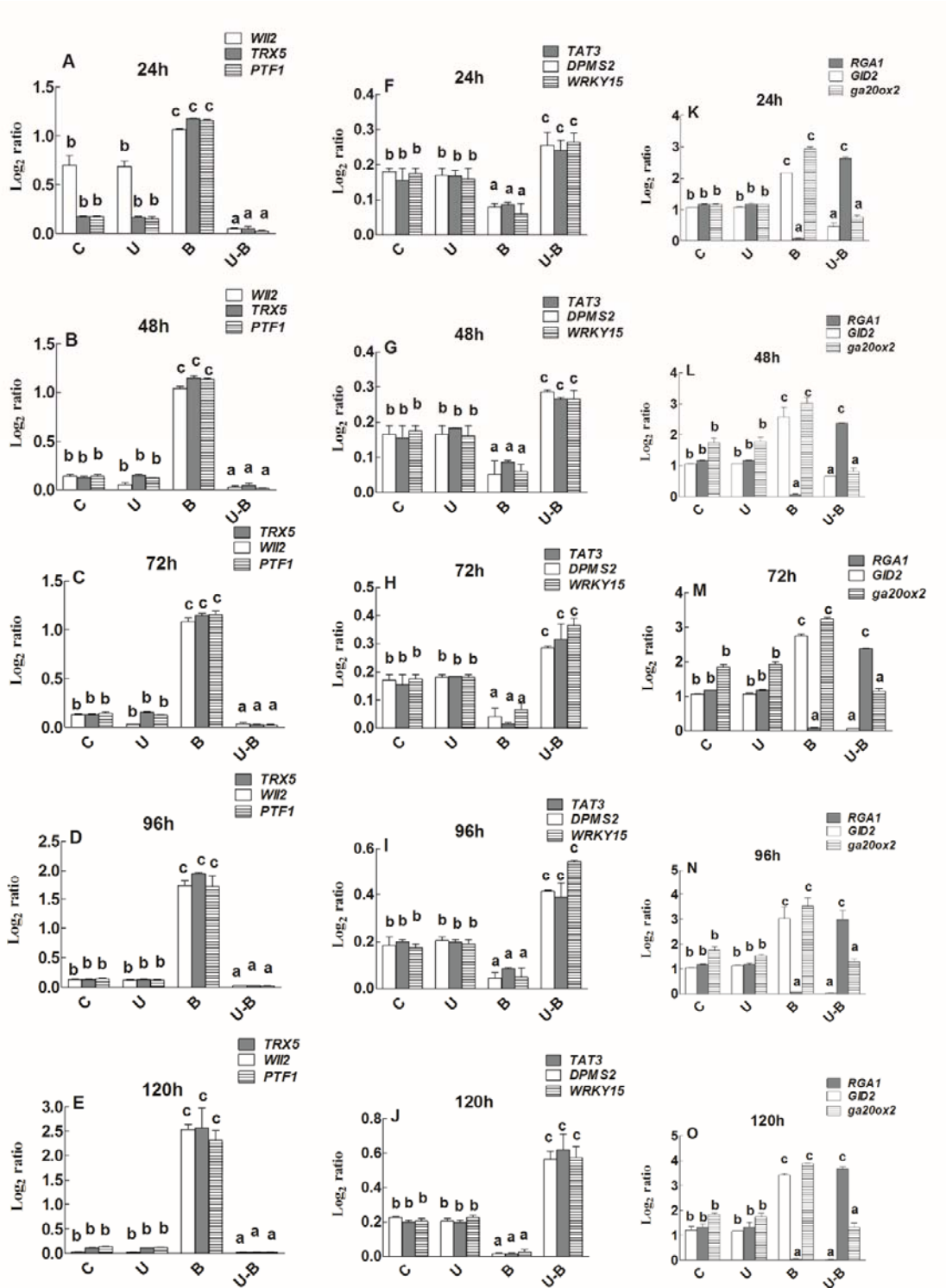
584 **Figure 9**

585 Data extracted from Expression Angler 2016 showing the set of co-expressed genes with *GID*

586 (a) and DELLA (*Mihailova et al.*) (b) under microbe stresses based on R- cut off range -0.7

587 to 0.9) with the principle gene expression.

588



589

590 **Figure 10**

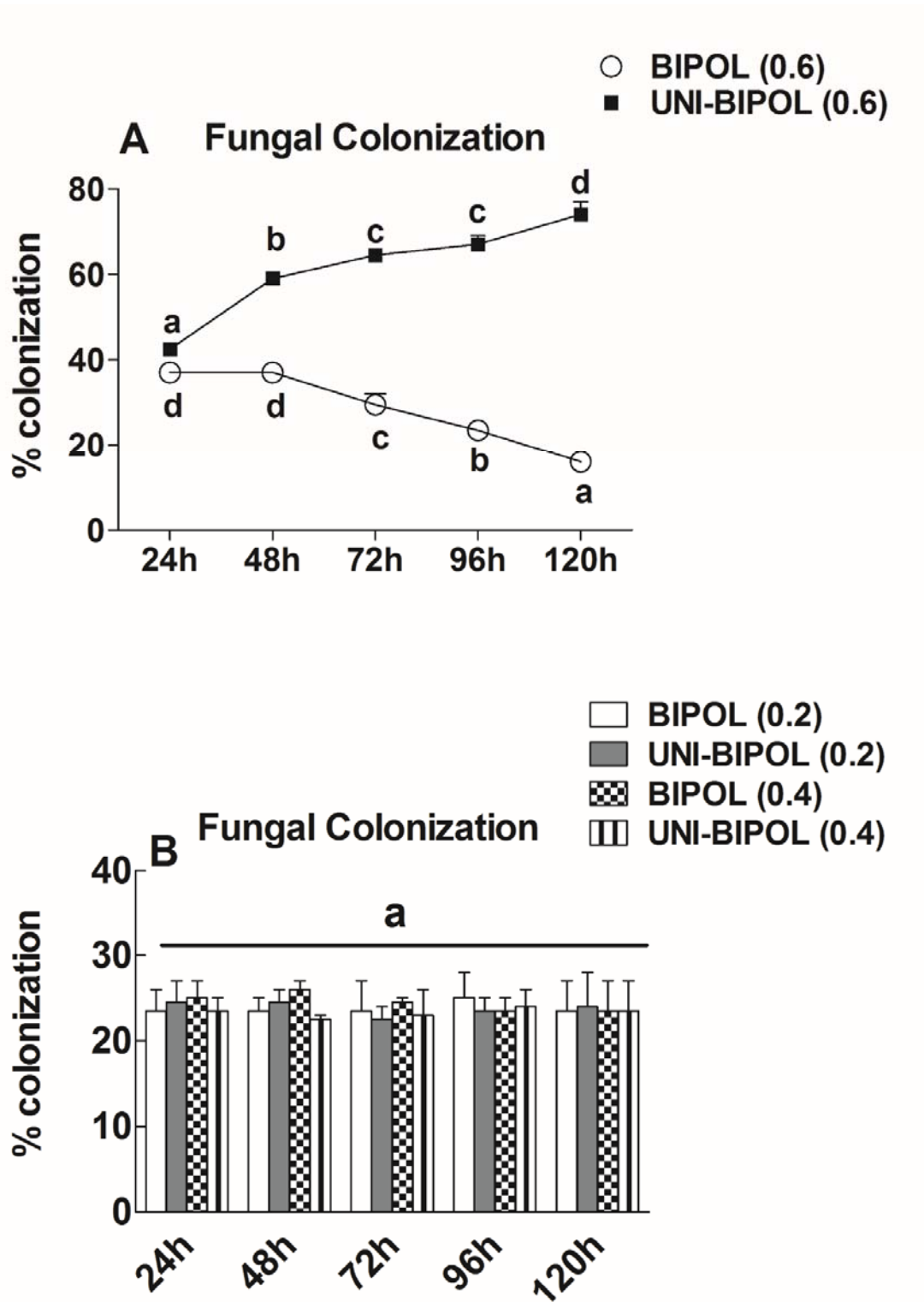
591 Determination of gene expression in the leaf tissues of 11 days old maize seedlings exposed

592 to different treatments including C (control); U (Uniconazole), B (BIPOL), U-B

593 (Uniconizole-BIPOL) for the different time duration. Duncan's test was performed and  
594 different alphabetic letters shows the significant difference. Experiment was repeated at least  
595 three time independently.

596

597



598 **Figure 11**

599 Determination of fungal colonization on maize root under the stress of BIPOL (BIPOL) and  
600 UNI-BIPOL (Uniconizole-BIPOL) in spore density ( $OD_{0.2}$ ,  $OD_{0.4}$  and  $OD_{0.6}$ ) on the roots of  
601 maize seedlings. Ducan's test was performed and different alphabetic letters shows the  
602 significant difference. Experiment was repeated at least three time independently.

603

604

605

606

607

608

609

610

611

612

613

614

615

616

617

618

619

620

621

622



624 **Discussion**

625 HR in plant is elicited in response to interaction of the host plant with the undesirable  
626 microbe (Ger and Chang, 2019). The microbe may be a pathogen or inert to the host plant  
627 (Hatsugai et al., 2018). When we applied BIPOL to the roots of maize 11 day old seedlings in  
628 hydroponic solution (Hassan), the seedlings elicited a HR. The HR deeply affected the  
629 growth and development of the seedlings. As the result, the B seedlings had low RGR and  
630 NAR. Accompanied by this, the seedlings also deterred the colonization of BIPOL at their  
631 roots. Interestingly, the seedlings elicited HR was limited to the BIPOL SD ( $OD_{0.6}$ ). There  
632 was no such response observed in BIPOL SD ( $OD_{0.2}$  or  $OD_{0.4}$ ). It clearly meant that the  
633 specific spore density of BIPOL could elicited a HR in host. Most of the pathogenic fungi  
634 undergo HR in host once in contact with host plant at maximum SD. We here concluded that  
635 BIPOL SD inducing HR is  $OD_{0.6}$ .

636 Most of plant hormones acting phyto signalling molecules aid the host plant to induce the HR  
637 during its interaction with undesirable microbe (Li et al., 2019). We observed high level of  
638  $GA_3$  in host leaf and root exudates after application of BIPOL SD ( $OD_{0.6}$ ) to the host roots.  
639 Interestingly, this high level of  $GA_3$  reduced the level of IAA and TZn in host leaf and root  
640 exudates which clearly indicated the high level of  $GA_3$  produced negative cross talks with  
641 IAA and TZn at the interaction of BIPOL We blocked the biosynthesis of  $GA_3$  for 72 hour of  
642 treatment by applying uniconazole to the leaf of 11 days old seedlings.  $GA_3$  is the growth  
643 plant hormones which induce cell elongation and division in maize plants (Zhang et al.,  
644 2019). Uniconazole treatment blocked  $GA_3$  biosynthesis at product level. As expected, the  
645 growth of the maize seedlings reduced significantly, determined by low RGR and NAR  
646 values. Surprisingly, in  $GA_3$  deficient environment, BIPOL SD ( $OD_{0.6}$ ) colonized the host  
647 root and promoted the growth. However, BIPOL SD ( $OD_{0.2}$  or  $OD_{0.4}$ ) could not promote  
648 growth in uniconazole treated seedlings. This clearly indicated that both SDs are not effective



649 either at pathogenic level or growth promoting level. We also examined the growth  
650 suppression of Uniconazole treated seedlings and BIPOL SD (OD<sub>0.6</sub>) treated seedling through  
651 the production of secondary metabolites in host leaf and root exudates. Plant produces  
652 secondary metabolites under biotic or abiotic stress to cope them at the expense of its normal  
653 growth and development (Yang et al., 2018). As expected, the level of Proline, TFC (total  
654 flavonoid content), PPs (phenylpropanoids) and GLs (Glucosinolates) were high in  
655 Uniconazole treated seedlings and BIPOL SD (OD<sub>0.6</sub>) treated seedling. However, after the  
656 release of Uniconazole effect on the maize seedlings, the level of secondary metabolites was  
657 lowered.

658 Several biotic or abiotic stresses induce oxidase activity in plants which in turn decrease  
659 growth of the host plant to eliminate the stress condition (Selinski et al., 2018). As expected,  
660 the treatment of uniconazole to maize seedlings increased oxidase activity and subsequently  
661 decreased plant growth till 72 hours after which the oxidase activity became normal.  
662 However, the oxidase activity remained high in BIPOL treatment SD (OD<sub>0.6</sub>) with co-related  
663 low growth rate of the seedlings. As opposed, high catalase activity was noted in prolifically  
664 growing seedlings (Poli et al., 2018). Similarly, we observed low growth in low catalase  
665 activity treatments (uniconazole till 72 hours and BIPOL SD (OD<sub>0.6</sub>) in all duration). In the  
666 contrary, BIPOL treatment SD (OD<sub>0.6</sub>).

667 On the contrary, BIPOL SD (OD<sub>0.6</sub>) treated seedling could not reduce the level of secondary  
668 metabolites was lowered. This literally meant that stress of BIPOL SD (OD<sub>0.6</sub>) treatment  
669 remained high during the treatment hours. Additionally, the host seedlings did not respond to  
670 BIPOL SD (OD<sub>0.2</sub> or OD<sub>0.4</sub>) due to normal secondary metabolites concentration in both leaf  
671 and root exudates. Similarly, the same treatments too did not reduce the high concentration of  
672 secondary metabolites in Uniconazole treated seedlings. We determined HR in host in host by  
673 quantifying the PA, pure OPDA, esterified OPDA, and JA levels in host under biotic and

674 abiotic stress (Schuman et al., 2018). As expected, the maize seedlings containing high  
675 concentration of GA<sub>3</sub> (B seedlings treated by BIPOL SD (OD<sub>0.6</sub>)) produced high level of HR  
676 inducing molecules while the seedlings containing low GA<sub>3</sub> level (U-B seedlings treated by  
677 BIPOL SD (OD<sub>0.2</sub> or OD<sub>0.4</sub>)) produced low concentration of these molecules. However, the  
678 other two SDs could not trigger the production of HR inducing molecules in neither in  
679 Uniconazole treated seedlings nor control seedlings.

680 This deduced that the two BIPOL SD (OD<sub>0.2</sub> or OD<sub>0.4</sub>)) treatment to maize seedlings are  
681 inert, neither growth promoting and virulent. The same pattern was also followed by HR  
682 signalling inducing molecules as c-di-GMP, and cAMP. In host plant under the interaction of  
683 undesirable microbe, several protease activities begin which break down the proteins involves  
684 in the transportation of nutrients and facilitation of microbial colonization (Havé et al., 2018).  
685 We determined three marker protease activities such as universal protease activity, serine  
686 protease activity and cysteine protease. The quantification of protease activities also showed  
687 high HR in the maize seedling stressed with BIPOL SD (OD<sub>0.6</sub>) only. As the HR triggered in  
688 host plant due to microbe interaction, cell death inducing substances are biosynthesized  
689 known as phytoalexins (Komives and Kiraly, 2019). We determined four phytoalexins  
690 commonly found in maize as Zealexins A4, kauralexin A4, DIMBOA and HDMBOA (Yang  
691 et al., 2019). As expected, the level these phytoalexins were high only in BIPOL SD (OD<sub>0.6</sub>)  
692 treatment.

693 Using in-silico approach, we finally extracted data regarding gene expressions in *A. thaliana*  
694 under the interaction with model biotrophs and necrotroph at GA<sub>3</sub> hypersensitivity. The  
695 expression of 9 markers genes were analysed in maize seedlings using qRT-PCR. The result  
696 showed that genes (*WII2*, *TRX5*, *PTF1*, *DPMS2*, *TAT3*, *WRKY15*, *GID1*, *ga20ox2* and *RGR1*)  
697 inhibiting microbe colonization in host were highly upregulated in the seedlings which had  
698 high GA<sub>3</sub> level (BIPOL treated seedlings). On the contrary, such genes were down regulated

699 in Y-B thus facilitating BIPOL interaction. The description of the genes were taken from the  
700 online available database of Arabidopsis (TAIR) (Consortium et al., 2019). After overall  
701 inspection, we also determined BIPOL colonization frequency on the roots of maize  
702 seedlings. During plant microbe interaction, roots of the most plant host provide optimal site  
703 for colonization (Hugoni et al., 2018). As expected, the BIPOL SD (OD<sub>0.6</sub>) colonized only in  
704 the roots of the uniconizole pre-treated seedlings of maize at leaf. It was because the level of  
705 GA<sub>3</sub> was inhibited which could interfered the colonization. Due to the inhibition of GA<sub>3</sub>, IAA  
706 and Transzeatin levels were high in the seedlings. IAA (Mehmood et al., 2018) and  
707 Tranzeatin (Kabbara et al., 2018) are involved to have a role in the accommodation of fungal  
708 colonization on host plant roots. As opposed, in the seedling of maize where GA<sub>3</sub> was high  
709 (control seedlings treated with BIPOL SD (OD<sub>0.6</sub>)), the BIPOL colonization was hindered.  
710 This could be due to the high level of GA<sub>3</sub> which developed cross talks with IAA and  
711 Tranzeatin, thus decreasing its production in host.

## 712 **Conclusion**

713 Beside growth inducing molecules, GA<sub>3</sub> also indicates the compatibility of host-micorbial  
714 interaction. Inoculation of BIPOL majorly caused GA<sub>3</sub> hypersensitivity at a SD (OD<sub>0.6</sub>) at 600  
715 nm. this hypersensitivity interfered the optimal level of IAA and Trans-zeatin in the host,  
716 thereby demoting growth of the seedlings. Once the GA<sub>3</sub> was inhibited using uniconizole  
717 treatment BIPOL SD (OD<sub>0.6</sub>) colonized on the seedlings root and resumed its growth  
718 promoting acitivity. This supported our hypothesis that GA<sub>3</sub> hypersensitivity hinders the  
719 interaction of BIPOL with *Z. mays* under its cross talks with IAA and trans-zeatin.

720

721

## Parsed Citations

**Aghajanzadeh TA, Prajapati DH, Burow M (2019) Copper toxicity affects indolic glucosinolates and gene expression of key enzymes for their biosynthesis in Chinese cabbage. Archives of Agronomy and Soil Science**

Pubmed: [Author and Title](#)

Google Scholar: [Author Only Title Only Author and Title](#)

**Almblad H, Rybtke M, Hendiani S, Andersen JB, Givskov M, Tolker-Nielsen T (2019) High levels of cAMP inhibit Pseudomonas aeruginosa biofilm formation through reduction of the c-di-GMP content. Microbiology 165: 324-333**

Pubmed: [Author and Title](#)

Google Scholar: [Author Only Title Only Author and Title](#)

**Amaral JS, Santos G, Oliveira MBP, Mafra I (2017) Quantitative detection of pork meat by EvaGreen real-time PCR to assess the authenticity of processed meat products. Food control 72: 53-61**

Pubmed: [Author and Title](#)

Google Scholar: [Author Only Title Only Author and Title](#)

**Asaf S, Khan AL, Waqas M, Kang S-M, Hamayun M, Lee I-J, Hussain A (2019) Growth-promoting bioactivities of Bipolaris sp. CSL-1 isolated from Cannabis sativa suggest a distinctive role in modifying host plant phenotypic plasticity and functions. Acta Physiologiae Plantarum 41: 65**

Pubmed: [Author and Title](#)

Google Scholar: [Author Only Title Only Author and Title](#)

**Asai S, Shirasu K (2015) Plant cells under siege: plant immune system versus pathogen effectors. Current opinion in plant biology 28: 1-8**

Pubmed: [Author and Title](#)

Google Scholar: [Author Only Title Only Author and Title](#)

**Bedini A, Mercy L, Schneider C, Franken P, Lucic-Mercy E (2018) Unravelling the initial plant hormone signalling, metabolic mechanisms and plant defense triggering the endomycorrhizal symbiosis behavior. Frontiers in plant science 9: 1800**

Pubmed: [Author and Title](#)

Google Scholar: [Author Only Title Only Author and Title](#)

**Bhatia SC (2018) Secondary Metabolites. In Plant Physiology, Development and Metabolism. Springer, pp 1099-1166**

Pubmed: [Author and Title](#)

Google Scholar: [Author Only Title Only Author and Title](#)

**Bheri M, Bhosle SM, Makandar R (2019) Shotgun proteomics provides an insight into pathogenesis-related proteins using anamorphic stage of the biotroph, Erysiphe pisi pathogen of garden pea. Microbiological research 222: 25-34**

Pubmed: [Author and Title](#)

Google Scholar: [Author Only Title Only Author and Title](#)

**Binenbaum J, Weinstain R, Shani E (2018) Gibberellin localization and transport in plants. Trends in plant science 23: 410-421**

Pubmed: [Author and Title](#)

Google Scholar: [Author Only Title Only Author and Title](#)

**Block AK, Vaughan MM, Schmelz EA, Christensen SA (2019) Biosynthesis and function of terpenoid defense compounds in maize (Zea mays). Planta 249: 21-30**

Pubmed: [Author and Title](#)

Google Scholar: [Author Only Title Only Author and Title](#)

**Body MJ, Neer WC, Vore C, Lin C-H, Vu DC, Schultz JC, Cocroft RB, Appel HM (2019) Caterpillar chewing vibrations cause changes in plant hormones and volatile emissions in Arabidopsis thaliana. Frontiers in plant science 10: 810**

Pubmed: [Author and Title](#)

Google Scholar: [Author Only Title Only Author and Title](#)

**Brumos J, Robles LM, Yun J, Vu TC, Jackson S, Alonso JM, Stepanova AN (2018) Local auxin biosynthesis is a key regulator of plant development. Developmental cell 47: 306-318. e305**

Pubmed: [Author and Title](#)

Google Scholar: [Author Only Title Only Author and Title](#)

**Bürger M, Chory J (2019) Stressed out about hormones: how plants orchestrate immunity. Cell host & microbe 26: 163-172**

Pubmed: [Author and Title](#)

Google Scholar: [Author Only Title Only Author and Title](#)

**Cadby IT, Basford SM, Nottingham R, Meek R, Lowry R, Lambert C, Tridgett M, Till R, Ahmad R, Fung R (2019) Nucleotide signaling pathway convergence in a cAMP-sensing bacterial c-di-GMP phosphodiesterase. The EMBO journal 38**

Pubmed: [Author and Title](#)

Google Scholar: [Author Only Title Only Author and Title](#)

**Ceh-Pavia E, Lu H (2016) Determination of the Redox Properties of Mitochondrial Sulphydryl Oxidase Erv1. Free Radical Biology and Medicine 100: S26-S27**

Pubmed: [Author and Title](#)

Google Scholar: [Author Only Title Only Author and Title](#)

**Chagas FO, de Cassia Pessotti R, Caraballo-Rodríguez AM, Pupo MT (2018) Chemical signaling involved in plant–microbe interactions. *Chemical Society Reviews* 47: 1652-1704**

Pubmed: [Author and Title](#)

Google Scholar: [Author Only](#) [Title Only](#) [Author and Title](#)

**Chaliha C, Rugen MD, Field RA, Kalita E (2018) Glycans as modulators of plant defense against filamentous pathogens. *Frontiers in plant science* 9: 928**

Pubmed: [Author and Title](#)

Google Scholar: [Author Only](#) [Title Only](#) [Author and Title](#)

**Consortium IAI, Doherty C, Friesner J, Gregory B, Loraine A, Megraw M, Provart N, Slotkin RK, Town C, Assmann SM (2019) Arabidopsis bioinformatics resources: The current state, challenges, and priorities for the future. *Plant Direct* 3: e00109**

Pubmed: [Author and Title](#)

Google Scholar: [Author Only](#) [Title Only](#) [Author and Title](#)

**Czerniawski P, Bednarek P (2018) Glutathione S-T transferases in the Biosynthesis of Sulfur-Containing Secondary Metabolites in Brassicaceae Plants. *Frontiers in Plant Science* 9**

Pubmed: [Author and Title](#)

Google Scholar: [Author Only](#) [Title Only](#) [Author and Title](#)

**Dhawan D, Gupta J (2017) Research Article Comparison of Different Solvents for Phytochemical Extraction Potential from Datura metel Plant Leaves. *Int. J. Biol. Chem* 11: 17-22**

Pubmed: [Author and Title](#)

Google Scholar: [Author Only](#) [Title Only](#) [Author and Title](#)

**Ding M, Liu W, Peng J, Liu X, Tang Y (2018) Simultaneous determination of seven preservatives in food by dispersive liquid-liquid microextraction coupled with gas chromatography-mass spectrometry. *Food chemistry* 269: 187-192**

Pubmed: [Author and Title](#)

Google Scholar: [Author Only](#) [Title Only](#) [Author and Title](#)

**Farooq MA, Saqib ZA, Akhtar J, Bakhat HF, Pasala R-K, Dietz K-J (2019) Protective role of silicon (Si) against combined stress of salinity and boron (B) toxicity by improving antioxidant enzymes activity in rice. *Silicon* 11: 2193-2197**

Pubmed: [Author and Title](#)

Google Scholar: [Author Only](#) [Title Only](#) [Author and Title](#)

**Feurtado JA, Kermodé AR (2018) A merging of paths: abscisic acid and hormonal cross-talk in the control of seed dormancy maintenance and alleviation. *Annual Plant Reviews online*: 176-223**

Pubmed: [Author and Title](#)

Google Scholar: [Author Only](#) [Title Only](#) [Author and Title](#)

**Fu Y, Sun X, Wang L, Chen S (2018) Pharmacokinetics and Tissue Distribution Study of Pinosylvin in Rats by Ultra-High-Performance Liquid Chromatography Coupled with Linear Trap Quadrupole Orbitrap Mass Spectrometry. *Evidence-Based Complementary and Alternative Medicine* 2018**

Pubmed: [Author and Title](#)

Google Scholar: [Author Only](#) [Title Only](#) [Author and Title](#)

**Fuentes L, Figueroa CR, Valdenegro M (2019) Recent Advances in Hormonal Regulation and Cross-Talk during Non-Climacteric Fruit Development and Ripening. *Horticulturae* 5: 45**

Pubmed: [Author and Title](#)

Google Scholar: [Author Only](#) [Title Only](#) [Author and Title](#)

**Genovese S, Epifano F, Fiorito S, Taddeo VA, Preziuso F, Fraternali D (2018) Modulation of the phenylpropanoid geranylation step in *Anethum graveolens* cultured calli by ferulic acid and umbelliferone. *Industrial crops and products* 117: 128-130**

Pubmed: [Author and Title](#)

Google Scholar: [Author Only](#) [Title Only](#) [Author and Title](#)

**Genva M, Akong FO, Andersson MX, Deleu M, Lins L, Fauconnier M-L (2019) New insights into the biosynthesis of esterified oxylipins and their involvement in plant defense and developmental mechanisms. *Phytochemistry Reviews* 18: 343-358**

Pubmed: [Author and Title](#)

Google Scholar: [Author Only](#) [Title Only](#) [Author and Title](#)

**Ger M-J, Chang H (2019) Bacterial Pathogen Resistance by HRAP (hypersensitive response assisting protein) in Tobacco. In 2019 國際學生學術論文研討會. 元培醫事科技大學**

Pubmed: [Author and Title](#)

Google Scholar: [Author Only](#) [Title Only](#) [Author and Title](#)

**Gil-Ramírez A, Pavo-Caballero C, Baeza E, Baenas N, Garcia-Viguera C, Marin FR, Soler-Rivas C (2016) Mushrooms do not contain flavonoids. *Journal of Functional Foods* 25: 1-13**

Pubmed: [Author and Title](#)

Google Scholar: [Author Only](#) [Title Only](#) [Author and Title](#)

**Großkinsky DK, van der Graaff E, Roitsch T (2016) Regulation of abiotic and biotic stress responses by plant hormones. *Plant pathogen resistance biotechnology* 131**

Pubmed: [Author and Title](#)

Google Scholar: [Author Only](#) [Title Only](#) [Author and Title](#)

**Hassan MM (2017) Improvement of in vitro date palm plantlet acclimatization rate with kinetin and Hoagland solution. In Date Palm Biotechnology Protocols Volume I. Springer, pp 185-200**

Pubmed: [Author and Title](#)

Google Scholar: [Author Only](#) [Title Only](#) [Author and Title](#)

**Hatsugai N, Nakatsuji A, Unten O, Ogasawara K, Kondo M, Nishimura M, Shimada T, Katagiri F, Hara-Nishimura I (2018) Involvement of Adapter Protein Complex 4 in hypersensitive cell death induced by avirulent bacteria. Plant physiology 176: 1824-1834**

Pubmed: [Author and Title](#)

Google Scholar: [Author Only](#) [Title Only](#) [Author and Title](#)

**Havé M, Balliau T, Cottyn-Boitte B, Déron E, Cueff G, Soulay F, Lornac A, Reichman P, Dissmeyer N, Avice J-C (2018) Increases in activity of proteasome and papain-like cysteine protease in Arabidopsis autophagy mutants: back-up compensatory effect or cell-death promoting effect? Journal of experimental botany 69: 1369-1385**

Pubmed: [Author and Title](#)

Google Scholar: [Author Only](#) [Title Only](#) [Author and Title](#)

**Hendling M, Pabinger S, Peters K, Wolff N, Conzemius R, Barišić I (2018) Oli2go: an automated multiplex oligonucleotide design tool. Nucleic acids research 46: W252-W256**

Pubmed: [Author and Title](#)

Google Scholar: [Author Only](#) [Title Only](#) [Author and Title](#)

**Hiruma K (2019) Roles of Plant-Derived Secondary Metabolites during Interactions with Pathogenic and Beneficial Microbes under Conditions of Environmental Stress. Microorganisms 7: 362**

Pubmed: [Author and Title](#)

Google Scholar: [Author Only](#) [Title Only](#) [Author and Title](#)

**Hoeghe S, Kopetzki E, Ostler D, Seeber S, Tiefenthaler G (2017) Rapid method for cloning and expression of cognate antibody variable region gene segments. In. Google Patents**

Pubmed: [Author and Title](#)

Google Scholar: [Author Only](#) [Title Only](#) [Author and Title](#)

**Holland CK, Jez JM (2018) Arabidopsis: the original plant chassis organism. Plant cell reports 37: 1359-1366**

Pubmed: [Author and Title](#)

Google Scholar: [Author Only](#) [Title Only](#) [Author and Title](#)

**Hou Q, Ufer G, Bartels D (2016) Lipid signalling in plant responses to abiotic stress. Plant, cell & environment 39: 1029-1048**

Pubmed: [Author and Title](#)

Google Scholar: [Author Only](#) [Title Only](#) [Author and Title](#)

**Hughes G, Pemberton R, Fielden P, Hart JP (2015) Development of a novel reagentless, screen-printed amperometric biosensor based on glutamate dehydrogenase and NAD<sup>+</sup>, integrated with multi-walled carbon nanotubes for the determination of glutamate in food and clinical applications. Sensors and Actuators B: Chemical 216: 614-621**

Pubmed: [Author and Title](#)

Google Scholar: [Author Only](#) [Title Only](#) [Author and Title](#)

**Hugoni M, Luis P, Guyonnet J, el Zahar Haichar F (2018) Plant host habitat and root exudates shape fungal diversity. Mycorrhiza 28: 451-463**

Pubmed: [Author and Title](#)

Google Scholar: [Author Only](#) [Title Only](#) [Author and Title](#)

**Huttenlocher A, Schoen TJ, Rosowski EE, Knox BP, Bennin D, Keller NP (2019) Imaging invasive fungal growth and inflammation in NADPH oxidase-deficient zebrafish. bioRxiv: 703728**

Pubmed: [Author and Title](#)

Google Scholar: [Author Only](#) [Title Only](#) [Author and Title](#)

**Jenal U, Reinders A, Lori C (2017) Cyclic di-GMP: second messenger extraordinaire. Nature Reviews Microbiology 15: 271**

Pubmed: [Author and Title](#)

Google Scholar: [Author Only](#) [Title Only](#) [Author and Title](#)

**Jeon J, Kim JK, Kim H, Kim YJ, Park YJ, Kim SJ, Kim C, Park SU (2018) Transcriptome analysis and metabolic profiling of green and red kale (*Brassica oleracea* var. *acephala*) seedlings. Food chemistry 241: 7-13**

Pubmed: [Author and Title](#)

Google Scholar: [Author Only](#) [Title Only](#) [Author and Title](#)

**Joshi R, Sahoo KK, Tripathi AK, Kumar R, Gupta BK, Pareek A, Singla-Pareek SL (2018) Knockdown of an inflorescence meristem-specific cytokinin oxidase—OsCKX2 in rice reduces yield penalty under salinity stress condition. Plant, cell & environment 41: 936-946**

Pubmed: [Author and Title](#)

Google Scholar: [Author Only](#) [Title Only](#) [Author and Title](#)

**Kabbara S, Schmölling T, Papon N (2018) CHASEing cytokinin receptors in plants, bacteria, fungi, and beyond. Trends in plant science 23: 179-181**

Pubmed: [Author and Title](#)

Google Scholar: [Author Only](#) [Title Only](#) [Author and Title](#)



**Khan A, Ali L, Hussain J, Rizvi T, Al-Harrasi A, Lee I-J (2015) Enzyme inhibitory radicicol derivative from endophytic fungus *Bipolaris sorokiniana* LK12, associated with *Rhazya stricta*. *Molecules* 20: 12198-12208**

Pubmed: [Author and Title](#)

Google Scholar: [Author Only](#) [Title Only](#) [Author and Title](#)

**Khan AR, Ullah I, Waqas M, Shahzad R, Hong S-J, Park G-S, Jung BK, Lee I-J, Shin J-H (2015) Plant growth-promoting potential of endophytic fungi isolated from *Solanum nigrum* leaves. *World Journal of Microbiology and Biotechnology* 31: 1461-1466**

Pubmed: [Author and Title](#)

Google Scholar: [Author Only](#) [Title Only](#) [Author and Title](#)

**Kim BM, Lotter-Stark HCT, Rybicki EP, Chikwamba RK, Palmer KE (2018) Characterization of the hypersensitive response-like cell death phenomenon induced by targeting antiviral lectin griffithsin to the secretory pathway. *Plant biotechnology journal* 16: 1811-1821**

Pubmed: [Author and Title](#)

Google Scholar: [Author Only](#) [Title Only](#) [Author and Title](#)

**Koch M, Busse M, Naumann M, Jákl B, Smit I, Cakmak I, Hermans C, Pawelzik E (2019) Differential effects of varied potassium and magnesium nutrition on production and partitioning of photoassimilates in potato plants. *Physiologia plantarum* 166: 921-935**

Pubmed: [Author and Title](#)

Google Scholar: [Author Only](#) [Title Only](#) [Author and Title](#)

**Kornives T, Kiraly Z (2019) Disease resistance in plants: The road to phytoalexins and beyond. *Ecocycles* 5: 7-12**

Pubmed: [Author and Title](#)

Google Scholar: [Author Only](#) [Title Only](#) [Author and Title](#)

**Kurosawa RdNF, Vivas M, Amaral ATd, Ribeiro RM, Miranda SB, Pena GF, Leite JT, Mora F (2018) Popcorn germplasm resistance to fungal diseases caused by *Exserohilum turcicum* and *Bipolaris maydis*. *Bragantia* 77: 36-47**

Pubmed: [Author and Title](#)

Google Scholar: [Author Only](#) [Title Only](#) [Author and Title](#)

**Lee MR, Kim CS, Park T, Choi Y-S, Lee K-H (2018) Optimization of the ninhydrin reaction and development of a multiwell plate-based high-throughput proline detection assay. *Analytical biochemistry* 556: 57-62**

Pubmed: [Author and Title](#)

Google Scholar: [Author Only](#) [Title Only](#) [Author and Title](#)

**Li R, Chen C, He J, Zhang L, Zhang L, Guo Y, Zhang W, Tan K, Huang J (2019) E3 ligase ASB8 promotes porcine reproductive and respiratory syndrome virus proliferation by stabilizing the viral Nsp1 $\alpha$  protein and degrading host IKK $\beta$  kinase. *Virology* 532: 55-68**

Pubmed: [Author and Title](#)

Google Scholar: [Author Only](#) [Title Only](#) [Author and Title](#)

**Li S, Zhao J, Zhai Y, Yuan Q, Zhang H, Wu X, Lu Y, Peng J, Sun Z, Lin L (2019) The hypersensitive induced reaction 3 (HIR 3) gene contributes to plant basal resistance via an EDS 1 and salicylic acid-dependent pathway. *The Plant Journal***

Pubmed: [Author and Title](#)

Google Scholar: [Author Only](#) [Title Only](#) [Author and Title](#)

**Lim G-H, Singhal R, Kachroo A, Kachroo P (2017) Fatty acid- and lipid-mediated signaling in plant defense. *Annual review of Phytopathology* 55: 505-536**

Pubmed: [Author and Title](#)

Google Scholar: [Author Only](#) [Title Only](#) [Author and Title](#)

**Luis A, Corpas FJ, López-Huertas E, Palma JM (2018) Plant superoxide dismutases: function under abiotic stress conditions. In *antioxidants and antioxidant enzymes in higher plants*. Springer, pp 1-26**

Pubmed: [Author and Title](#)

Google Scholar: [Author Only](#) [Title Only](#) [Author and Title](#)

**Mamontova T, Afonin AM, Ihling C, Soboleva A, Lukasheva E, Sulima AS, Shtark OY, Akhtemova GA, Povydysh MN, Sinz A (2019) Profiling of Seed Proteome in Pea (*Pisum sativum* L.) Lines Characterized with High and Low Responsivity to Combined Inoculation with Nodule Bacteria and Arbuscular Mycorrhizal Fungi. *Molecules* 24: 1603**

Pubmed: [Author and Title](#)

Google Scholar: [Author Only](#) [Title Only](#) [Author and Title](#)

**Matić S, Pegoraro M, Noris E (2016) The C2 protein of tomato yellow leaf curl Sardinia virus acts as a pathogenicity determinant and a 16-amino acid domain is responsible for inducing a hypersensitive response in plants. *Virus research* 215: 12-19**

Pubmed: [Author and Title](#)

Google Scholar: [Author Only](#) [Title Only](#) [Author and Title](#)

**McDonald MC, Ahren D, Simpfendorfer S, Milgate A, Solomon PS (2018) The discovery of the virulence gene ToxA in the wheat and barley pathogen *Bipolaris sorokiniana*. *Molecular plant pathology* 19: 432-439**

Pubmed: [Author and Title](#)

Google Scholar: [Author Only](#) [Title Only](#) [Author and Title](#)

**McGuinness PN, Reid JB, Foo E (2019) The role of gibberellins and brassinosteroids in nodulation and arbuscular mycorrhizal associations. *Frontiers in Plant Science* 10**

Pubmed: [Author and Title](#)

Google Scholar: [Author Only](#) [Title Only](#) [Author and Title](#)

**Mehmood A, Hussain A, Irshad M, Khan N, Hamayun M, Ismail, Afridi SG, Lee I-J (2018) IAA and flavonoids modulates the association between maize roots and phyto-stimulant endophytic *Aspergillus fumigatus* greenish. Journal of plant interactions 13: 532-542**

Pubmed: [Author and Title](#)

Google Scholar: [Author Only](#) [Title Only](#) [Author and Title](#)

**Mihailova G, Kocheva K, Goltsev V, Kalaji HM, Georgieva K (2018) Application of a diffusion model to measure ion leakage of resurrection plant leaves undergoing desiccation. Plant physiology and biochemistry 125: 185-192**

Pubmed: [Author and Title](#)

Google Scholar: [Author Only](#) [Title Only](#) [Author and Title](#)

**Mirabet V, Krupinski P, Hamant O, Meyerowitz EM, Jönsson H, Boudaoud A (2018) The self-organization of plant microtubules inside the cell volume yields their cortical localization, stable alignment, and sensitivity to external cues. PLoS computational biology 14: e1006011**

Pubmed: [Author and Title](#)

Google Scholar: [Author Only](#) [Title Only](#) [Author and Title](#)

**Mott GA, Desveaux D, Guttman DS (2018) A high-sensitivity, microtiter-based plate assay for plant pattern-triggered immunity. Molecular plant-microbe interactions 31: 499-504**

Pubmed: [Author and Title](#)

Google Scholar: [Author Only](#) [Title Only](#) [Author and Title](#)

**Müller C, Elliott J, Chryssanthacopoulos J, Arneth A, Balkovic J, Ciais P, Deryng D, Folberth C, Glotter M, Hoek S (2017) Global gridded crop model evaluation: benchmarking, skills, deficiencies and implications. Geoscientific Model Development Discussions 10: 1403-1422**

Pubmed: [Author and Title](#)

Google Scholar: [Author Only](#) [Title Only](#) [Author and Title](#)

**Nandhini M, Rajini S, Udayashankar A, Niranjana S, Lund OS, Shetty H, Prakash H (2018) Diversity, plant growth promoting and downy mildew disease suppression potential of cultivable endophytic fungal communities associated with pearl millet. Biological control 127: 127-138**

Pubmed: [Author and Title](#)

Google Scholar: [Author Only](#) [Title Only](#) [Author and Title](#)

**Narusaka M, Narusaka Y (2017) Thienopyrimidine-type compounds protect Arabidopsis plants against the hemibiotrophic fungal pathogen *Colletotrichum higginsianum* and bacterial pathogen *Pseudomonas syringae* pv. *maculicola*. Plant signaling & behavior 12: e1293222**

Pubmed: [Author and Title](#)

Google Scholar: [Author Only](#) [Title Only](#) [Author and Title](#)

**Nur Ain Izzati M, Madihah M, Nor Azizah K, Najihah A, Muskhazli M (2019) First Report of *Bipolaris cactivora* Causing Brown Leaf Spot in Rice in Malaysia. Plant Disease 103: 1021**

Pubmed: [Author and Title](#)

Google Scholar: [Author Only](#) [Title Only](#) [Author and Title](#)

**Obata T (2019) Metabolons in plant primary and secondary metabolism. Phytochemistry Reviews: 1-25**

Pubmed: [Author and Title](#)

Google Scholar: [Author Only](#) [Title Only](#) [Author and Title](#)

**Orrego F, Ortiz-Calderón C, Lutts S, Ginocchio R (2019) Growth and physiological effects of single and combined Cu, NaCl, and water stresses on *Atriplex atacamensis* and *A. halimus*. Environmental and Experimental Botany: 103919**

Pubmed: [Author and Title](#)

Google Scholar: [Author Only](#) [Title Only](#) [Author and Title](#)

**Petrasch S, Knapp SJ, Van Kan JA, Blanco-Ulate B (2019) Grey mould of strawberry, a devastating disease caused by the ubiquitous necrotrophic fungal pathogen *Botrytis cinerea*. Molecular plant pathology**

Pubmed: [Author and Title](#)

Google Scholar: [Author Only](#) [Title Only](#) [Author and Title](#)

**Pitsili E, Phukan UJ, Coll NS (2019) Cell Death in Plant Immunity. Cold Spring Harbor Perspectives in Biology: a036483**

Pubmed: [Author and Title](#)

Google Scholar: [Author Only](#) [Title Only](#) [Author and Title](#)

**Poli Y, Nallamothu V, Balakrishnan DB, Palakurthi R, Desiraju S, Mangrauthia SK, Voleti SR, Neelamraju S (2018) Increased catalase activity and maintenance of Photosystem II distinguishes high-yield mutants from low-yield mutants of rice var. Nagina22 under low-phosphorus stress. Frontiers in plant science 9: 1543**

Pubmed: [Author and Title](#)

Google Scholar: [Author Only](#) [Title Only](#) [Author and Title](#)

**Portwood JL, Woodhouse MR, Cannon EK, Gardiner JM, Harper LC, Schaeffer ML, Walsh JR, Sen TZ, Cho KT, Schott DA (2018) MaizeGDB 2018: the maize multi-genome genetics and genomics database. Nucleic acids research 47: D1146-D1154**

Pubmed: [Author and Title](#)

Google Scholar: [Author Only](#) [Title Only](#) [Author and Title](#)

**Ramirez-Prado JS, Abulfaraj AA, Rayapuram N, Benhamed M, Hirt H (2018) Plant immunity: from signaling to epigenetic control of**



**defense. Trends in plant science 23: 833-844**

Pubmed: [Author and Title](#)

Google Scholar: [Author Only Title Only Author and Title](#)

**Reissmann N, Muddukrishna A (2018) Diagnosing Highly-Parallel OpenMP Programs with Aggregated Grain Graphs. In European Conference on Parallel Processing. Springer, pp 106-119**

Pubmed: [Author and Title](#)

Google Scholar: [Author Only Title Only Author and Title](#)

**Röcker J, Schmitt M, Pasch L, Ebert K, Grossmann M (2016) The use of glucose oxidase and catalase for the enzymatic reduction of the potential ethanol content in wine. Food chemistry 210: 660-670**

Pubmed: [Author and Title](#)

Google Scholar: [Author Only Title Only Author and Title](#)

**Schuman MC, Meldau S, Gaquereel E, Diezel C, McGale E, Greenfield S, Baldwin IT (2018) The active jasmonate JA-ILE regulates a specific subset of plant jasmonate-mediated resistance to herbivores in nature. Frontiers in plant science 9: 787**

Pubmed: [Author and Title](#)

Google Scholar: [Author Only Title Only Author and Title](#)

**Selinski J, Scheibe R, Day DA, Whelan J (2018) Alternative oxidase is positive for plant performance. Trends in plant science 23: 588-597**

Pubmed: [Author and Title](#)

Google Scholar: [Author Only Title Only Author and Title](#)

**Selvakumar G, Shagol C, Kang Y, Chung B, Han S, Sa T (2018) Arbuscular mycorrhizal fungi spore propagation using single spore as starter inoculum and a plant host. Journal of applied microbiology 124: 1556-1565**

Pubmed: [Author and Title](#)

Google Scholar: [Author Only Title Only Author and Title](#)

**Sen MK, Jamal M, Nasrin S (2013) Sterilization factors affect seed germination and proliferation of *Achyranthes aspera* cultured in vitro. Environmental and Experimental Biology 11: 119-123**

Pubmed: [Author and Title](#)

Google Scholar: [Author Only Title Only Author and Title](#)

**Silva FLB, Vieira LGE, Ribas AF, Moro AL, Neris DM, Pacheco AC (2018) Proline accumulation induces the production of total phenolics in transgenic tobacco plants under water deficit without increasing the G6PDH activity. Theoretical and Experimental Plant Physiology 30: 251-260**

Pubmed: [Author and Title](#)

Google Scholar: [Author Only Title Only Author and Title](#)

**Speijer D (2019) Can All Major ROS Forming Sites of the Respiratory Chain Be Activated By High FADH2/NADH Ratios? Ancient evolutionary constraints determine mitochondrial ROS formation. BioEssays 41: 1800180**

Pubmed: [Author and Title](#)

Google Scholar: [Author Only Title Only Author and Title](#)

**Srikantam S, Arumugam G (2019) Hydroalcoholic extract of licorice (*Glycyrrhiza glabra* L.) root attenuates ethanol and cerulein induced pancreatitis in rats. Asian Pacific Journal of Tropical Biomedicine 9: 424**

Pubmed: [Author and Title](#)

Google Scholar: [Author Only Title Only Author and Title](#)

**Suárez I, da Silva Lima G, Conti R, Pinedo C, Moraga J, Barúa J, de Oliveira ALL, Aleu J, Durán-Patrón R, Macías-Sánchez AJ (2018) Structural and biosynthetic studies on eremophilinols related to the phytoalexin capsidiol, produced by *Botrytis cinerea*. Phytochemistry 154: 10-18**

Pubmed: [Author and Title](#)

Google Scholar: [Author Only Title Only Author and Title](#)

**Terrón-Camero LC, Molina-Moya E, Sanz-Fernández M, Sandalio LM, Romero-Puertas MC (2018) Detection of reactive oxygen and nitrogen species (ROS/RNS) during hypersensitive cell death. In Plant Programmed Cell Death. Springer, pp 97-105**

Pubmed: [Author and Title](#)

Google Scholar: [Author Only Title Only Author and Title](#)

**Tijero V, Teribia N, Munné-Bosch S (2019) Hormonal Profiling Reveals a Hormonal Cross-Talk During Fruit Decay in Sweet Cherries. Journal of Plant Growth Regulation 38: 431-437**

Pubmed: [Author and Title](#)

Google Scholar: [Author Only Title Only Author and Title](#)

**Tohge T, Borghi M, Fernie AR (2018) The natural variance of the *Arabidopsis* floral secondary metabolites. Scientific Data 5: 180051**

Pubmed: [Author and Title](#)

Google Scholar: [Author Only Title Only Author and Title](#)

**Vasseur F, Bresson J, Wang G, Schwab R, Weigel D (2018) Image-based methods for phenotyping growth dynamics and fitness components in *Arabidopsis thaliana*. Plant methods 14: 63**

Pubmed: [Author and Title](#)

Google Scholar: [Author Only Title Only Author and Title](#)

**Wahyuningsih S, Wulandari L, Wartono M, Munawaroh H, Ramelan A (2017) The effect of pH and color stability of anthocyanin on food colorant. In IOP Conference Series: Materials Science and Engineering, Vol 193. IOP Publishing, p 012047**

Pubmed: [Author and Title](#)

Google Scholar: [Author Only](#) [Title Only](#) [Author and Title](#)

**Xiang H, Okamura H, Kezuka Y, Katoh E (2018) Physical and thermodynamic characterization of the rice gibberellin receptor/gibberellin/DELLA protein complex. Scientific reports 8**

Pubmed: [Author and Title](#)

Google Scholar: [Author Only](#) [Title Only](#) [Author and Title](#)

**Yang L, Wen K-S, Ruan X, Zhao Y-X, Wei F, Wang Q (2018) Response of plant secondary metabolites to environmental factors. Molecules 23: 762**

Pubmed: [Author and Title](#)

Google Scholar: [Author Only](#) [Title Only](#) [Author and Title](#)

**Yang P, Praz C, Li B, Singla J, Robert CA, Kessel B, Scheuermann D, Lüthi L, Ouzunova M, Erb M (2019) Fungal resistance mediated by maize wall-associated kinase Zm WAK-RLK 1 correlates with reduced benzoxazinoid content. New Phytologist 221: 976-987**

Pubmed: [Author and Title](#)

Google Scholar: [Author Only](#) [Title Only](#) [Author and Title](#)

**Yimer HZ, Nahar K, Kyndt T, Haeck A, Van Meulebroek L, Vanhaecke L, Demestere K, Höfte M, Gheysen G (2018) Gibberellin antagonizes jasmonate-induced defense against *Meloidogyne graminicola* in rice. New Phytologist 218: 646-660**

Pubmed: [Author and Title](#)

Google Scholar: [Author Only](#) [Title Only](#) [Author and Title](#)

**Yin J, Xu T, Zhang N, Wang H (2016) Three-enzyme cascade bioreactor for rapid digestion of genomic DNA into single nucleosides. Analytical chemistry 88: 7730-7737**

Pubmed: [Author and Title](#)

Google Scholar: [Author Only](#) [Title Only](#) [Author and Title](#)

**Zhang S, Yang R, Huo Y, Liu S, Yang G, Huang J, Zheng C, Wu C (2018) Expression of cotton PLATZ1 in transgenic *Arabidopsis* reduces sensitivity to osmotic and salt stress for germination and seedling establishment associated with modification of the abscisic acid, gibberellin, and ethylene signalling pathways. BMC plant biology 18: 218**

Pubmed: [Author and Title](#)

Google Scholar: [Author Only](#) [Title Only](#) [Author and Title](#)

**Zhang X, Wang B, Zhao Y, Zhang J, Li Z (2019) Auxin and GA signaling play important roles in the maize response to phosphate deficiency. Plant Science 283: 177-188**

Pubmed: [Author and Title](#)

Google Scholar: [Author Only](#) [Title Only](#) [Author and Title](#)

**Zheng H, Liu Y, Zhang J, Chen Y, Yang L, Li H, Wang L (2018) Factors influencing soil enzyme activity in China's forest ecosystems. Plant ecology 219: 31-44**

Pubmed: [Author and Title](#)

Google Scholar: [Author Only](#) [Title Only](#) [Author and Title](#)

**Zhou J, Jin J, Li X, Zhao Z, Zhang L, Wang Q, Li J, Zhang Q, Xiang S (2018) Total flavonoids of *Desmodium styracifolium* attenuates the formation of hydroxy-L-proline-induced calcium oxalate urolithiasis in rats. Urolithiasis 46: 231-241**

Pubmed: [Author and Title](#)

Google Scholar: [Author Only](#) [Title Only](#) [Author and Title](#)

**Zuluaga AP, Vega-Arreguín JC, Fei Z, Ponnala L, Lee SJ, Matas AJ, Patev S, Fry WE, Rose JK (2016) Transcriptional dynamics of *Phytophthora infestans* during sequential stages of hemibiotrophic infection of tomato. Molecular plant pathology 17: 29-41**

Pubmed: [Author and Title](#)

Google Scholar: [Author Only](#) [Title Only](#) [Author and Title](#)